# ANTHROPOGENIC, BIOGENIC AND PYROGENIC EMISSION SOURCES AND ATMOSPHERIC FORMALDEHYDE (HCHO) AND NITROGEN DIOXIDE ($NO_2$) COLUMNS OVER DIFFERENT LANDUSE/LANDCOVERS OF SOUTH ASIA

RANA, A. D.[1] – PARVEZ, S.[1] – UL-HAQ, Z.[1*] – BATOOL, S. A.[1] – CHAUDHARY, M. N.[2] – MAHMOOD, K.[1] – TARIQ, S.[1]

[1]*Remote Sensing and GIS Group, Department of Space Science, University of the Punjab, Lahore, Pakistan*

[2]*Institute of Geology, University of the Punjab, Lahore, Pakistan*

**Corresponding author*
*e-mail: zia.spsc@yahoo.com; phone: + 92-301-435-2543*

(Received 27th Mar 2019; accepted 2nd Jul 2019)

**Abstract.** This study presents spatiotemporal variability of two important air pollutants, Formaldehyde (HCHO) and Nitrogen dioxide ($NO_2$), concomitant to underlying anthropogenic, biogenic and pyrogenic emission sources from different landuse/landcovers over South Asia, from 2005-2016, using OMI sensor onboard Aura satellite. Annual and seasonal spatial distributions for both the gases reveal that trends of change are linked with landuse/landcovers of different geographical regions of South Asia. Annual distribution of $NO_2$ shows a negative trend from 2012-2016, with annual decrease of ~1.06% in comparison to a rise, from 2005-2011 at a rate of ~1.86%/year. Analyzing seven study zones, distinctively identifies higher-emissions for both the gases from anthropogenic sources, in zones, 2,3,4 and 6, highlighting, emissions from megacities of Pakistan (Lahore, Faisalabad), India (Delhi, Kolkata, Lucknow) and Bangladesh (Dhaka), mainly due to urbanization, power-generation plants and mining-activities. Episodes of pyrogenic-emissions dominate seasonally in zones2 and 4, due to crop residue burning from Punjab plains of Pakistan and India and zone5 from Bangladesh and Myanmar. Isoprene, a precursor to HCHO is one of its main biogenic sources and higher emissions of HCHO dominate in zones3 and 7 with deciduous forests of lower Himalayas in northwest and Western Ghats in southwest India. In zones 4,5 HCHO emissions are dictated by isoprene emissions from Sundarbans in Bangladesh and palm-oil-plantations in Myanmar.
**Keywords:** *trace gases, OMI, spatiotemporal analysis, isoprene, remote sensing*

**Abbreviations:** ACCMIP: Atmospheric Chemistry and Climate Model Intercomparison Project; BVOCs: Biogenic Volatile Organic Compounds; $CH_4$: Methane; CityZEN: megaCITY- Zoom for the Environment; CO: Carbon Monoxide; ECCAD: Emissions of atmospheric Compounds & Compilation of Ancillary Data; GOME: Global Ozone Monitoring Experiment; HCHO: Formaldehyde; IGB: Indo-Gangetic Basin; MACCity: Monitoring Atmospheric Composition and Climate/CityZEN EU projects; MODIS: Moderate Resolution Imaging Spectroradiometer; NASA: National Aeronautics and Space Administration; NCEP: National Centers for Environmental Prediction; NDVI: Normalized Difference Vegetation Index; NMVOCs: Non-Methane Volatile Organic Compounds; NOx: Nitrogen Oxides; $NO_2$: Nitrogen Dioxide; $O_3$: Ozone; OH: Hydroxyl Radicals; OMI: Ozone Monitoring Instrument; SAARC: South Asian Association for Regional Cooperation; SCIAMACHY SCanning Imaging Absorption spectroMeter for Atmospheric CHartographY; Terra: Earth observing satellite system Launched by NASA; UV: Ultra Violet; UV-Vis: Ultraviolet to Visible; VOCs: Volatile Organic Compounds

## Introduction

In the troposphere, Formaldehyde (HCHO) exists everywhere as a short-lived indoor and outdoor pollutant with a lifetime of few hours during the daylight (Sander et al., 2006). It is a carcinogenic pollutant, affecting the tropospheric photochemistry (Hassan


http://www.aloki.hu ● ISSN 1589 1623 (Print) ● ISSN 1785 0037 (Online)
DOI: http://dx.doi.org/10.15666/aeer/1705_1098911015

et al., 2018) and U.S. Environmental Protection Agency has declared, HCHO as the most important carcinogen in the outdoor air and is identified amongst the 187 hazardous air pollutants (Zhu et al., 2017; Zhang et al., 2018) Main source of tropospheric HCHO is oxidation of methane ($CH_4$) by Hydroxyl (OH) radicals. Whereas, short lived Non-Methane Volatile Organic Compounds (NMVOC) like alkanes, alkenes, aromatic hydrocarbons, and isoprene as a source of oxidation, dominate Methane in the continental boundary layer and contribute significantly to tropospheric HCHO concentrations. Ecologically, predictable and broadly defined trends for the isoprene dominance have been established as a Biogenic Volatile Organic Compounds (BVOC) over monoterpene. Isoprene as one of the BVOC after oxidation produces HCHO as a major product, and describes the temperature variations as a dominant variable at ecosystem level (Harrison et al., 2013). These temperature variations in the bigger context of climate change also affect the natural emissions of Volatile Organic Compounds (VOCs), like the emission of isoprene from vegetation (US-EPA, 2009). HCHO in the atmosphere is also contributed by vegetation (Lathiere et al., 2006), biomass burning processes and fuel combustion (Lee et al., 1998) in lesser content than oxidation. In midlatitude and forest cover of tropical regions, Isoprene as a VOC is the major precursor of HCHO (Palmer et al., 2003, 2006; Barkley et al., 2008; Curci et al., 2010).

Atmospheric oxidation of VOCs produces HCHO in large amounts, that can be detected through space as a total column by solar UV backscatter (Chance et al., 2000). Monitoring and recording of observations for HCHO columns from space started with the launch of the Global Ozone Monitoring Experiment (GOME) instrument in 1995 (Chance et al., 2000). Detection of HCHO columns using remote sensing data have been successfully used as a proxy for the identification of biogenic repositories and emissions of VOCs from the underlying sources (Palmer et al., 2003; Millet et al., 2008; Stavrakou et al., 2009; Marais et al., 2012; Barkley et al., 2013; Bauwens et al., 2016), pyrogenic sources (Shim et al., 2005; Gonzi et al., 2011) and anthropogenic sources (Fu et al., 2007; Marais et al., 2014; Zhu et al., 2014; Souri et al., 2017). Long term trends of HCHO column data have been analyzed by (De Smedt et al., 2010, 2015) with the help of GOME instrument and with the succeeding satellites like GOME-2, Ozone Monitoring Instrument (OMI) and Scanning Imaging Absorption Spectrometer for Atmospheric Cartography (SCIAMACHY).

In a recent study by (Zhu et al., 2018) using Ozone Monitoring Instrument (OMI) onboard Aura satellite, observing HCHO concentration over china for a period of 2005-2015, have observed strong seasonal pattern existing for high concentrations of HCHO in the summer season. At regional scale, increase has also been observed in the HCHO column for a period of 2005 to 2010 while, a decrease has been observed from 2010-2015. In addition to this, (Zhu et al., 2018) have also found that urban areas exhibit higher concentrations of HCHO column and increase has been observed for the emissions from industrial sources along with the similar emissions from residential sources. In summer times it has been concluded, that, anthropogenic VOCs contribute to high emissions along with the isoprene emissions.

In the atmosphere, nitrogen dioxide ($NO_2$) is considered as a highly reactive gas (US-EPA, 1998). Nitrogen oxides ($NO_x = NO + NO_2$), especially $NO_2$ in the atmosphere, has been observed to have adverse impacts on both, the human health and on the natural environment (Case et al., 1979; Barck et al., 2005). Another important aspect of the presence of $NO_x$ in the atmosphere is that these gases and hydrocarbons are correlated


http://www.aloki.hu ● ISSN 1589 1623 (Print) ● ISSN 1785 0037 (Online)
DOI: http://dx.doi.org/10.15666/aeer/1705_1098911015

with the surface level ozone (Varotsos et al., 1992). The tropospheric $NO_2$ pollution is greatly influenced by the spatial patterns of socio-economic conditions of certain geographical regions as well as it is affected by the changes in meteorological conditions, and also can be attributed to the topographic attributes, defined by the elevation, land use and land cover of the area under investigation (Parra et al., 2009). Emissions of $NO_2$ along with the other trace gases in Indo-Gangetic Plain (IGP) can be specifically associated with the agricultural landuse/landcover. As, significant emissions of $NO_2$, CO, $CO_2$, $CH_4$, and aerosol have been observed from the crop residue burning of both rice, wheat and from rice paddies as well (Ali et al., 2014; ul-Haq et al., 2014; Tariq and Ali, 2015). Keeping in view the environmental perspective, in South Asia, Pakistan is facing severe environmental problems due to rapid urbanization, with the need for more industrialization and motorization, energy crises and deforestation, leading to raised emissions of $NO_2$ (ul-Haq et al., 2017, 2018).

Atmospheric $NO_2$ and HCHO both have spectral absorption signatures in Ultraviolet to Visible (UV-Vis) regions of electromagnetic spectrum and are observed through the satellite sensors like OMI. These two pollutants have become of central importance and core data products, even for the future satellite-based programs for monitoring air quality (Nowlaqn et al., 2018). In a study, by (Zhu et al., 2017), emissions of HCHO produced through the oxidation of biogenically produced isoprene are linked with the concentrations of ($NO_x \equiv NO + NO_2$) in the atmosphere. Another important linkage, observed in the study by (Zhu et al., 2017), is between the absence of anthropogenic emissions of $NO_x$ and a reduction observed in the emissions of HCHO. Presence of these two gases as indoor and outdoor pollutants has also been established as a health risk, and in a study by (Maroziene and Grazuleviciene, 2002), low birth weight and preterm births have been observed to have some linkage with the maternal exposures during first trimester to ambient HCHO and $NO_2$ exposures respectively. According to a study, controlling the emissions of $NO_2$ is beneficial to both, environment and human health, as it improves the quality of the air with ozone and also reduces the risks of cancer related to HCHO emissions (Zhu et al., 2017).

The objectives of this study are to analyze spatiotemporal trends of tropospheric HCHO and $NO_2$ columns over South Asia for a temporal window of 12 years, from 2005-2016, with the help of remote sensing data from Ozone Monitoring Instrument (OMI) aboard the NASA Aura spacecraft. Interannual variability and seasonal trend analyses with spatial landuse/landcover pockets in varying scales and diversity of the landforms, influencing and modeling the local columns of HCHO and $NO_2$ will be analyzed. Some of the major biogenic activities on the global scale are affecting biogenic emissions of VOCs, as tropical deforestation has resulted in 29% decrease in isoprene emissions (Lathière et al., 2006). Assessment of the emission of the subject trace gases, affected by the underlying landuse/landcover in connection with anthropogenic, biogenic and pyrogenic activities is important to understand the atmospheric processes and photochemistry shaping up the overall atmospheric profile in this part of the world. For an in-depth analysis, to analyze the impact and trends of change on local HCHO and $NO_2$ columns, seven study zones will be analyzed for the assessment of emissions from different landuse/landcover directly or indirectly impacting tropospheric columns of HCHO and $NO_2$.


http://www.aloki.hu ● ISSN 1589 1623 (Print) ● ISSN 1785 0037 (Online)
DOI: http://dx.doi.org/10.15666/aeer/1705_1098911015

## Material and methods

### *Geography and meteorology of study area*

South Asia refers to the Southern region of the Asian continent with the most densely populated countries of the world, comprising of sub-Himalayan member states of South Asian Association for Regional Cooperation (SAARC), including Pakistan, India, Bhutan, Maldives, Sri Lanka, Afghanistan, Bangladesh and Nepal (Joshi, 2015) shown in *Figure 1a*. This region is marked in North by three gigantic mountain ranges of Himalaya, Hindukush and Karakoram, with emanating thickly populated, major river basins of Indus, Ganges, Brahmaputra, and Meghna extending from Pakistan to Bangladesh. The driest and deserted Baluchistan plateau located in Afghanistan and Pakistan, while the Peninsular India, consisting of Deccan plateau and the island countries of Sri Lanka and Maldives (Seligman, 2008; UNEP, 2008).

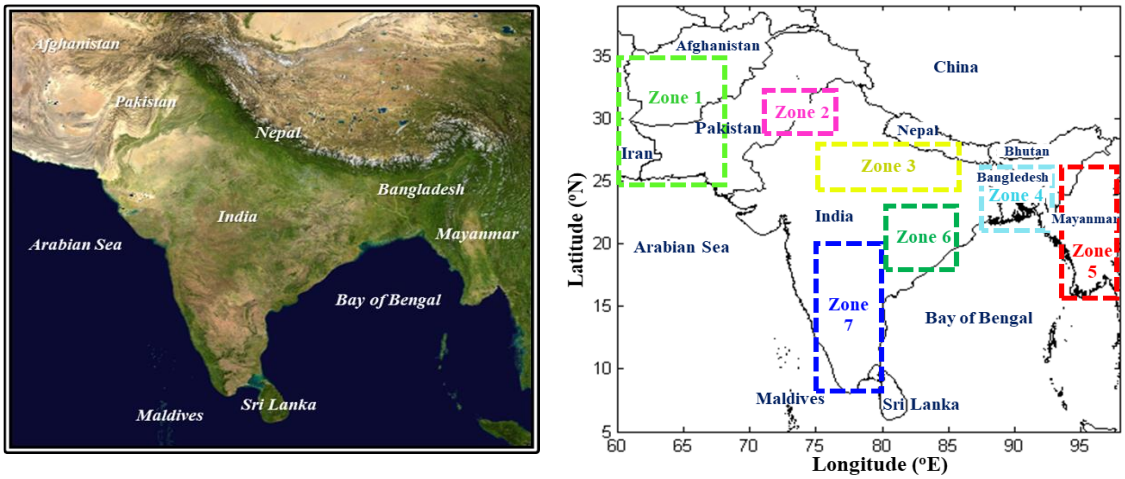


**a** **b**

***Figure 1.*** *(a) Satellite image map of South Asia showing landuse/landcover of world's most densely populated region. (Source: https://upload.wikimedia.org/wikipedia/commons/2/2a/Asia_satellite_orthographic.jpg), (b) Map of South Asia showing country boundaries and selected seven study zones shown in different colors*

South Asian climate is quite variant, dictated by highest mountains of the world, exhibiting arctic temperatures, transitioning in temperate regions in lower Himalayas to the tropical scenarios in Deccan plateau in the central India. Alternating wet and dry weather sessions brought by the monsoons control the overall climate of South Asia. Wet monsoons are caused by the moist winds from the sea in summertime, while in winter the dry monsoon is associated with the dry winds blowing out from land areas (UNEP, 2008; Joshi, 2015). For an in-depth analysis and investigation of HCHO and $NO_2$ along with the processes, South Asian region has been further investigated in seven study zones (*Fig. 1b*), from zone-1 to zone-7, comprising of regions with different landuse/landcovers, representatives of anthropogenic, biogenic and pyrogenic activities and emissions taking place at different scales. These seven study zones with corresponding geographic locations and possible/prominent sources of HCHO and $NO_2$ emissions from different landuse/landcovers and related activities have been detailed in *Table 1*.


http://www.aloki.hu ● ISSN 1589 1623 (Print) ● ISSN 1785 0037 (Online)
DOI: http://dx.doi.org/10.15666/aeer/1705_1098911015

***Table 1.*** *Study zones with geographical locations and prominent landuse/landcover sources of emissions of HCHO and $NO_2$. (Source: Lathière et al., 2010; Tariq et al., 2015; Sippo et al., 2016)*

| Study zones | Geographical bounding | Prominent landuse/landcover sources of $NO_2$ | Prominent landuse/landcover sources of HCHO |
|---|---|---|---|
| Zone-1 | 25-35 °N, 60-68 °E | Karachi, Gawadar and Chahbhar Ports activities, fossil fuel burning, urban (megacity Karachi) | Karachi, Gawadar and Chahbhar Ports activities, fossil fuel burning, urban (megacity Karachi), Shipping activity and emissions |
| Zone-2 | 28-32 °N, 72-77 °E | Large scale crop-residue burning, (post-monsoon and pre-monsoon pyrogenic emissions), Agricultural Landuse/Landcover, urban (megacities Lahore, Delhi, Faisalabad), industries, home heating, brick kilns, power plants | Large scale crop-residue burning (post-monsoon and pre-monsoon), urban (megacities Lahore, Delhi, Faisalabad), industries, home heating, brick kilns, power plants, deciduous forests in lower Himalayas in North Western parts of India (Biogenic emissions) |
| Zone-3 | 24-28 °N, 75-87 °E | Crop-residue burning (post-monsoon and pre-monsoon pyrogenic emissions), industries, home heating, brick kilns, power plants | Crop-residue burning (post-monsoon and pre-monsoon pyrogenic emissions), industries, home heating, brick kilns, power plants. Deciduous forests in sub-Himalayan Siwalik ranges in India and Nepal |
| Zone-4 | 20-26 °N, 87-92 °E | Large scale crop-residue burning (pre-monsoon pyrogenic emissions), Mining activities, power plants, industries, brick kilns, urban (megacities Dhaka, Kolkata, Anthropogenic emissions) | Large scale crop-residue burning (pre-monsoon), Mining activities, power plants, industries, brick kilns, urban (megacities Dhaka, Kolkata) Biogenic emissions from the mangroves of Sundarbans in Bangladesh |
| Zone-5 | 15-26 °N, 93-98 °E | Large scale crop-residue burning (pre-monsoon), fossil fuel burning, home heating | Large scale crop-residue burning (pre-monsoon), fossil fuel burning, home heating, Biogenic emissions from Palm oil plantations in Myanmar |
| Zone-6 | 18-23 °N, 80-85°E | Major coal powered energy production plants and the largest coal mining region of India | Major coal powered energy production plants and the largest coal mining region of India |
| Zone-7 | 08-20°N, 75-80 °E | South Western Ghats of India, Anthropogenic emissions from the mega city of Bengaluru | South Western Ghats of India with deciduous montane rain forests in Kerala, and Karnataka states of India, Anthropogenic emissions from the mega city of Bengaluru |

Maps of relative humidity at 925 mb, surface precipitation, wind vector at 925 mb and surface air temperature for South Asia for study period from 2005 to 2016 have been shown in *Figure 2*. These maps of selected meteorological parameters show the variations captured for four seasons i.e. winter season, comprising of the months of December, January and February, Pre-monsoon, described by March, April and May, Monsoon season, studied for the months of June, July and August, and Post-monsoon season consisting of the months of September, October and November. These


http://www.aloki.hu ● ISSN 1589 1623 (Print) ● ISSN 1785 0037 (Online)
DOI: http://dx.doi.org/10.15666/aeer/1705_1098911015

parameters have been mapped using records from NCEP–Reanalysis data from NOAA/OAR/ESRL PSD, Boulder, Colorado, USA. *http://www.esrl.noaa.gov/psd/.*

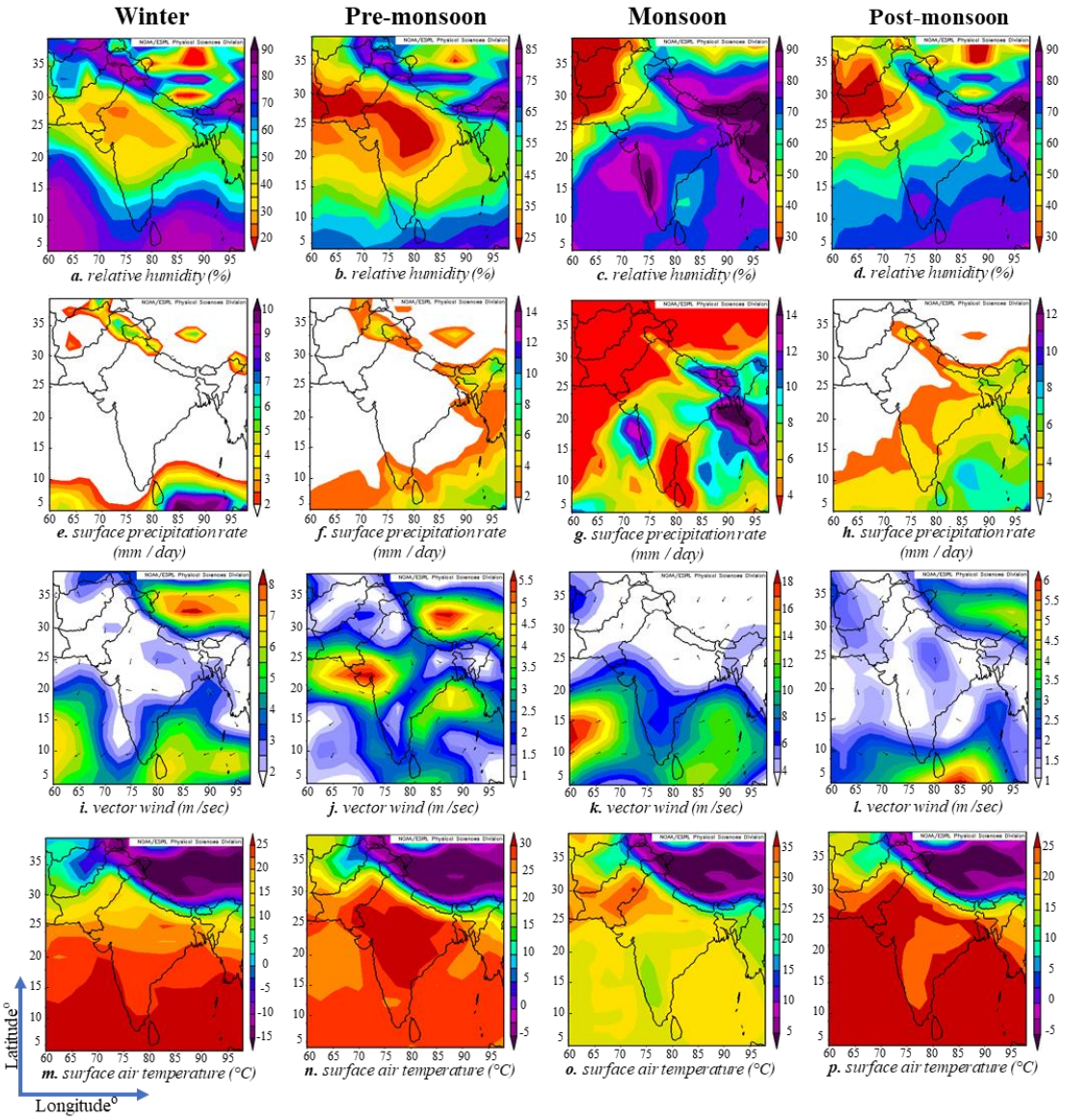


***Figure 2.*** *Maps showing seasonal composite means for the study period (2005-2016) of relative humidity (%) at 925 mb (a–d), surface precipitation rate (mm/day) (e–h), vector wind (m s-1) at 925 mb (i–l), and surface air temperature (°C) (m–p) over South Asia. Source: NOAA/ESRL Physical Sciences Division, Boulder Colorado from their Web site at http://www.esrl.noaa.gov/psd/*

Maps show the highest relative humidity in monsoon season for most of South Asia, especially on the Eastern regions, comprising of Bangladesh, Myanmar and central India along with the coastal belt in the Southeastern parts of India besides the Western Ghats. However, the winter season has been found dry over South Asia for having the minimum relative humidity for the study period. Monsoon season also dominates the


http://www.aloki.hu ● ISSN 1589 1623 (Print) ● ISSN 1785 0037 (Online)
DOI: http://dx.doi.org/10.15666/aeer/1705_1098911015

surface precipitation over South Asia, with few pockets of precipitations observed over the Himalayas in the winter season.

Pre-monsoon season highlights the high content of winds, especially in the mid latitude areas of South Asia, rising from the Runn of Kutch along the India Pakistan coastal border and in the Rajhistan desert. High wind vectors are also observed in Tibetan plateau in the pre-monsoon season. A consistent cold pattern can be observed all along the Himalayas, throughout the year in all four seasons in the maps showing the low surface air temperatures for the study period. Whereas, pre-monsoon and post-monsoon seasons exhibit high temperatures in mid latitudes to the southern parts of South Asia. Changes observed in the concentrations of tropospheric $NO_2$ column over South Asia could possibly be linked to the shifts in meteorological regimes controlled by the meteorological phenomenon, which result in the changes in the rates of chemical reactions in the troposphere (Voulgarakis et al., 2010).

### *NCEP/NCAR reanalysis data*

In 1991, a reanalysis1 project between National Center for Environmental Prediction (NCEP) and National Center for Atmospheric Research (NCAR) started to expand the National Meteorological Center (NMC)'s Climate Data Assimilation System (CDAS) project capacity. Objective of the CDAS project was to improve the forecasts by NMC operational Global Data Assimilation System (GDAS) over the last decade for the apparent climate change. In this reanalysis project a frozen state-of-the-art analysis and forecast system is used for the assimilation of the past data to perform reanalysis from 1957 to present. For the futuristic development in CDAS, same frozen state-of-the-art analysis/forecast system will be used to assess the anomalies in the current climate in the context of long reanalysis with the same data assimilation system (Kalnay et al., 1996). An improved version of reanalysis 1(R1) has been developed by NCEP/NCAR as Reanalysis 2 (R2). Improvements in R1 include updates in the model with better parameterization, inclusion of additional data and fixing the errors in assorted data assimilation. Data from NCEP/NCAR can be downloaded for more than 80 meteorological variables like, Surface temperature, Relative humidity, geopotential height, u-and v- wind components etc. Data from these sources are gridded and archived at the grid interval of 2.5° × 2.5° providing global data and is available from https://www.esrl.noaa.gov/psd/data/reanalysis/reanalysis.shtml.

### *OMI data for $NO_2$ and HCHO*

Ozone Monitoring Instrument (OMI) is a joint venture of Dutch-Finnish collaboration (Levelt et al., 2006) onboard NASA's EOS Aura satellite, launched in July 2004. OMI is a push-broom near-UV/Visible spectrometer orbiting in a sun-synchronous orbit with an ascending node, crossing the equator at 13:40 local time. OMI sensor captures data of various trace gases including $NO_2$ and HCHO. OMI scanner consists of two 2-dimensional Charged Coupled Devices (CCD) detectors (Dobber et al., 2006). To sync the spectral and spatial registration, one of the two CCDs, i.e. CCD1 captures the UV1 (264-311 nm) and UV2 (264-311 nm), while CCD2 captures the VIS (349-504 nm) spectral bands. Spectral features of $NO_2$ are more prominent in the later channel, while UV2 spectral channel is used for HCHO slant column densities (SCDs) (Zara et al., 2018). OMI sensor captures the global data daily with spatial resolutions of 13 × 24 $km^2$ to ~25 × 105 $km^2$ in nadir and to the outermost


http://www.aloki.hu ● ISSN 1589 1623 (Print) ● ISSN 1785 0037 (Online)
DOI: http://dx.doi.org/10.15666/aeer/1705_1098911015

swath-angle, respectively with a swath of 2600 km at every given exposure in the orbit (De Graaf et al., 2016; Krotkov et al., 2016).

*OMI tropospheric HCHO data*

OMI sensor has been in orbit for more than a decade, and its long-term observations of tropospheric HCHO column has provided valuable information regarding this important trace gas carcinogen. HCHO column data used in this study has a grid interval of 0.25° latitude by 0.25° longitude, retrieved through Differential Optical Absorption Spectroscopy (DOAS) algorithm and an Intermediate Model of the Global and Annual Evolution of Species (IMAGES) as a priori information (Kaczorowski and Perelli, 2004). OMI sensor also provides a valuable difference in time window, providing a complimentary early afternoon data of tropospheric HCHO column at 13:40 local solar time (Kurosu, 2008; Millet et al., 2008) as compared to the other satellites, like GOME-2 at 9:30 and SCIAMACHY at 10:00 local solar time providing the HCHO column data at mid-morning (Chance et al., 2000; Palmer et al., 2001; De Smedt et al., 2008). The Royal Belgian Institute for Space Aeronomy (BIRA-IASB), in the previous version addressed the instrumental degradation and the striping effect by employing row-dependent background normalization (De Smedt et al., 2015). Several improvements in the product also include accounting for more accurately the absorption of $O_2$-$O_2$. For this purpose, interactive DOAS algorithm involving three fitting intervals was used. In order to reduce the degradation, radiances in remote equatorial Pacific were used (De Smedt et al., 2015). In the previous products, some of the main reasons of uncertainty, ranging from 30 to 40% in the tropospheric HCHO column include, errors in retrieval of the SCD and errors in estimation of Air Mass Factor (AMF) (De Smedt et al., 2008), where AMF has been defined as the ratio of SCD and VCD (Millet et al., 2006). Therefore, the HCHO products available on (TEMIS) are highly applicable for the spatial and temporal assessment of HCHO distributions over South Asia in the context of regional landuse/landcover. In this study, daily, global, gridded (OMHCHOd) Level-3 data for tropospheric HCHO Vertical Column Density (VCD) has been used for the study period of twelve years, i.e. 2005-2016, obtained from Tropospheric Emission Monitoring Internet Service (TEMIS) (http://h2co.aeronomie.be/).

*OMI tropospheric $NO_2$ data*

NASA's EOS Aura satellite with OMI sensor was launched in July 2004, and provides a daily, global gridded coverage of tropospheric concentrations of $NO_2$. For retrievals of $NO_2$ the cloud conditions used, have taken into account the cloud cover to be clear and up to 30% in Air Mass Factor (AMF), that uses the Lambertian Cloud Model with an assumed albedo of 0.8 to develop a simulated profile of $NO_2$ (Stammes et al., 2008). Radiative transfer models are used to calculate the AMFs, which considers the parameters like, surface albedo, cloud and aerosol properties, optical geometry, vertical distribution of absorbing trace gas and atmospheric scattering by air molecules (Bucsela et al., 2006; Stammes et al., 2008; Boersma et al., 2011). For the estimation of $NO_2$ Slant Column Densities (SCDs) to retrieve the vertical $NO_2$ column, Differential Optical Absorption Spectroscopy (DOAS) spectral fitting, with radiance in the range of 405-465 nm has been used. In order to get the Vertical Column Density (VCD) of a gas, SCD, depending upon density of the gas and various other parameters is divided by the


http://www.aloki.hu ● ISSN 1589 1623 (Print) ● ISSN 1785 0037 (Online)
DOI: http://dx.doi.org/10.15666/aeer/1705_1098911015

AMF. Improvement in $NO_2$ retrievals can be achieved by curtailing the errors introduced in calculating AMF, due to surface albedo, presence of clouds and $NO_2$ profile as the dominant anomalous factors, affecting the accurate tropospheric $NO_2$ retrievals over areas with enhanced $NO_2$ (Boersma et al., 2004). Uncertainties in surface albedo contribute 20-30%, while, for cloud fraction it may contribute as high as 20-50% errors for the estimation of $NO_2$ column (Boersma et al., 2004). Another factor contributing to the inaccurate estimates of $NO_2$ are aerosols, that can indirectly affect the calculations for the AMF, as they introduce uncertainties in the cloud fraction calculations (Boersma et al., 2008, 2009). A comparison of ground-based in-situ measurements and the data retrieved from OMI sensor suggests that the data from OMI sensor is 0-30% biased (Lamsal et al., 2010). In this study, OMI sensor product (OMNO2d v003) for tropospheric $NO_2$ column prepared at level-3, providing the data in gridded form at a grid interval of 0.25° latitude by 0.25° longitude is used and downloaded from Giovanni, https://giovanni.gsfc.nasa.gov/.

### *MACCity emissions data*

MACCity is a joint data product contributed by two projects namely, Monitoring Atmospheric Composition and Climate (MACC) and megaCITY–Zoom for the Environment (CityZEN). MACCity products deliver emission data for various atmospheric gasses for the last about sixty years, from 1960 to 2020 and is provided by Emissions of atmospheric Compounds & Compilation of Ancillary Data (ECCAD). MACCity anthropogenic emission datasets are based on Representative Concentration Pathways (RCPs, 8.5, van Vuuren et al., 2011) and Atmospheric Chemistry and Climate Model Inter-comparison Project ACCMIP, (Lamarque et al., 2010). For the futuristic projections of emissions for different scenarios used in the IPCC AR5 report (van Vuuren et al., 2011), starting point for the development of the RCPs is based on the ACCMIP emissions in year, 2000. Whereas, anthropogenic emissions inventoried through ACCMIP rely on various emission database inventories combined and synchronized together, including RETRO, EDGAR, EMEP, EPA, REAS, GICC and GFEDv2, which are based on emission estimates due to anthropogenic activities, historical emissions databases, modelled studies and satellite observations. Many modelers name the MACCity as A2-ACCMIP for having some minor differences between A2-ACCMIP (AeroCom Phase II-ACCMIP) and MACCity (Diehl et al., 2012). MACCity anthropogenic emission datasets are available for download from Ether/ECCAD databases, provided at *http://www.eccad.sedoo.fr*.

In this study, MACCity data for HCHO and $NO_x$ emissions gridded at 0.5° latitude by 0.5° longitude (Granier et al., 2011) have been analyzed for the study period of 12 years, i.e. from 2005 to 2016, generated through six different anthropogenic emission sectors, including industrial sector (for both non-combustion and combustion), waste burning from agricultural fields, residential emissions, energy production sector, transportation sector and an overall sumsector (Amnuaylojaroen et al., 2014).

## Analysis and discussion

### *MACCity HCHO emissions*

Spatial distributions of MACCity HCHO emission data from different emission sectors for South Asia spanning over a period of 12 years, from 2005 to 2016 are shown


http://www.aloki.hu ● ISSN 1589 1623 (Print) ● ISSN 1785 0037 (Online)
DOI: http://dx.doi.org/10.15666/aeer/1705_1098911015

in *Figure 3*. Spatial representation of sum emissions due to anthropogenic activities contributed by some of the major emission sources are shown in *Figure 3a*. These major contributors to the sum sector include emissions from agricultural waste, residential and commercial practices, from industrial processes, transportation sector and from energy production and distribution sectors as shown in *Figure 3*.

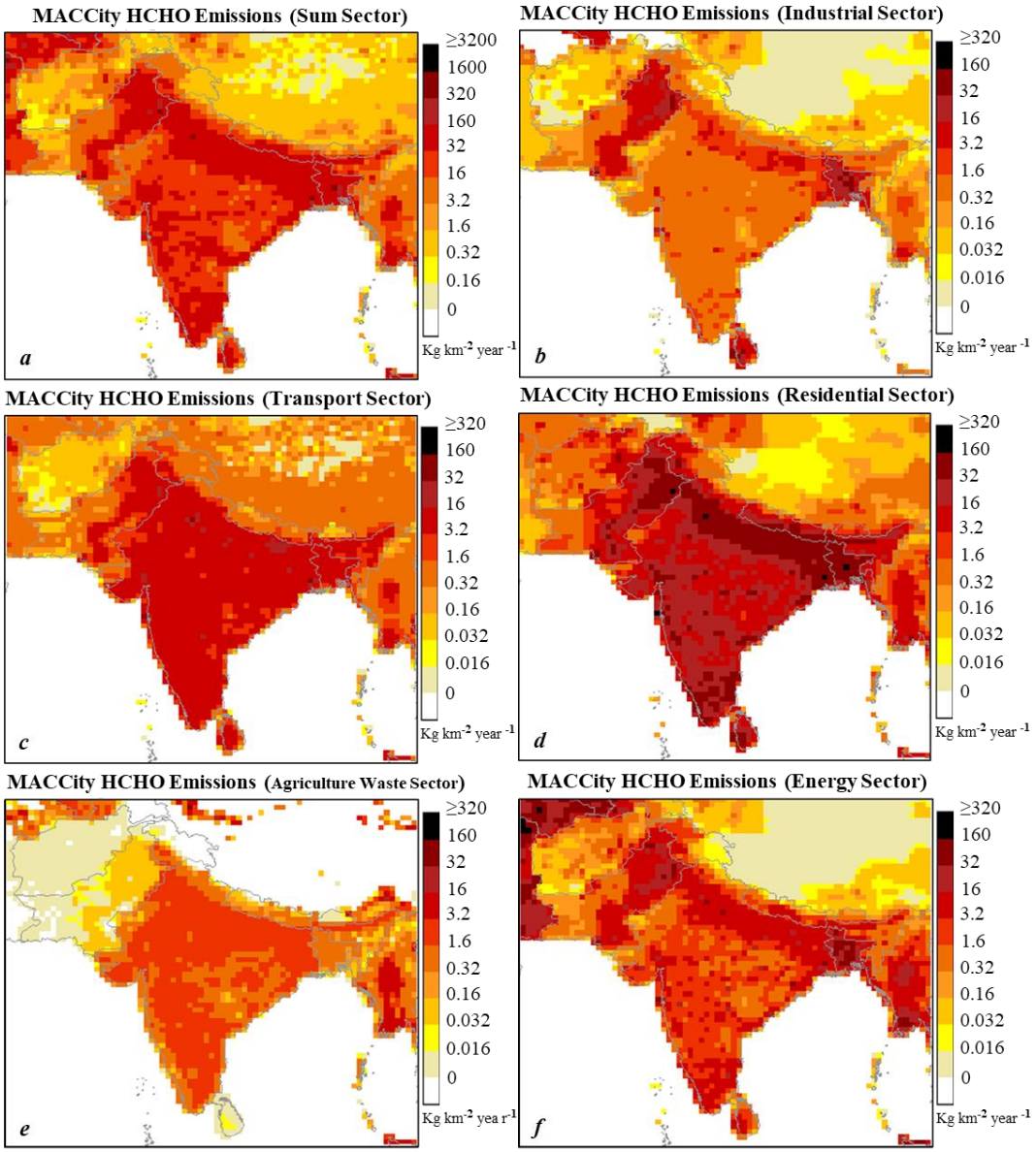


***Figure 3.*** *MACCity based average anthropogenic HCHO emissions (kg km$^{-2}$ year$^{-1}$) from (a) Sum sector (b) Industrial sector (c) Transport sector (d) Residential sector (e) Agricultural Waste sector and (f) Energy sector over South Asia during 2005-2016*

As shown in *Table 2*, MACCity HCHO anthropogenic emission datasets have shown a considerable rise in emissions from transportation sector in South Asia, raising the emissions from ~8536 kg km$^{-2}$ year$^{-1}$ in 2005 to ~12322 kg km$^{-2}$ year$^{-1}$ in 2016. A


http://www.aloki.hu ● ISSN 1589 1623 (Print) ● ISSN 1785 0037 (Online)
DOI: http://dx.doi.org/10.15666/aeer/1705_1098911015

statistical linear regression-based change analysis on annual mean data of 12 years (2005-2016), shows, ~51% rise in the emissions from transportation sector with ($R^2$ = 0.74). Like the transportation sector, residential and energy sectors also show significant rises, i.e. 13.8% and 11.5% respectively derived through regression-based trend analysis of 12 years of the study period with corresponding coefficients of determination ($R^2$ = 0.72 and 0.62) respectively. Anthropogenic emissions of HCHO are generally observed to be on a rise during the study period and overall sum sector emissions are raised by 21.6% with coefficient of determination ($R^2$ = 0.86) over South Asia. According to (Surl et al., 2018), these high emissions of HCHO from NMVOCs may be associated with the origination from the stationary combustion sources like, residential areas and also from the transportation sectors. In this study, high percentage changes observed in the transportation and residential sectors during the study period 2005-2016 are also endorsed by the observations in the foresaid study.

***Table 2.*** *MACCity average anthropogenic emissions of HCHO in (kg km$^{-2}$ year$^{-1}$), percentage change, slope of the regression equation and coefficient of determination $R^2$ over South Asia from January 2005 to December 2016*

| **Emission sectors** | **Average emissions kg km$^{-2}$ year$^{-1}$ (2005-2016)** | **% Change (2005-2016)** | **(Slope of regression equation); (Coefficient of determination $R^2$)** |
|---|---|---|---|
| Sum sector | 72740 | 21.6 | (1234.2 ± 146.6); (0.86) |
| Agricultural waste sector | 2611 | 7.5 | (17.1 ± 5.1); (0.53) |
| Energy sector | 17207 | 11.5 | (169.9 ± 40.9); (0.62) |
| Industrial sector | 4759 | 3.5 | (14.9 ± 6.2); (0.36) |
| Residential sector | 38909 | 13.8 | (457.3 ± 88.4); (0.72) |
| Transportation sector | 9397 | 51.1 | (347.7 ± 65.2); (0.74) |

### *MACCity $NO_x$ emissions*

Spatial distributions of MACCity $NO_x$ emissions from different emission sources for the study region over a period of 12 years, from 2005 to 2016 are shown in *Figure 4*. Spatial representation of sum emissions due to anthropogenic activities contributed by some of the major emission sources in South Asia are shown in *Figure 4a.* Major contributors to the sum sector include emissions from residential and commercial practices, from industrial processes, from agricultural waste, transportation sector and from energy production and distribution sectors as shown in *Figure 4.*

As given in *Table 3*, MACCity $NO_x$ anthropogenic emission datasets have shown a considerable rise in the emissions from the transportation sector in South Asia for the study period of 12 years. Emissions in this sector vary from ~ 573947 kg km$^{-2}$ year$^{-1}$ in year 2005 to ~ 1120025 kg km$^{-2}$ year$^{-1}$ in 2016, making a drastic rise in emissions to about 95.6% with a coefficient of determination ($R^2$ = 0.98), through a linear regression trend analysis. This rise is also consistent with the rise in emissions of HCHO for transportation sector showing the largest change in anthropogenic emissions with an increase of ~51% for the study period. Like the transportation sector, energy and industrial sectors also show significant rises in the emissions of $NO_x$, i.e. 35.3% and 20.7% respectively with the corresponding coefficient of determination ($R^2$ = 0.94 and 0.97) determined through regression analysis for the entire study period of 12 years.


http://www.aloki.hu ● ISSN 1589 1623 (Print) ● ISSN 1785 0037 (Online)
DOI: http://dx.doi.org/10.15666/aeer/1705_1098911015

Anthropogenic emissions of $NO_x$ are generally on a rise as observed by the overall sum sector emissions raised by 42.7% having a coefficient of determination ($R^2$ = 0.99). In this study, these high emissions of $NO_x$ may be associated with the overall high emissions recorded for the tropospheric HCHO column as well, and as reported by Surl et al. (2018).

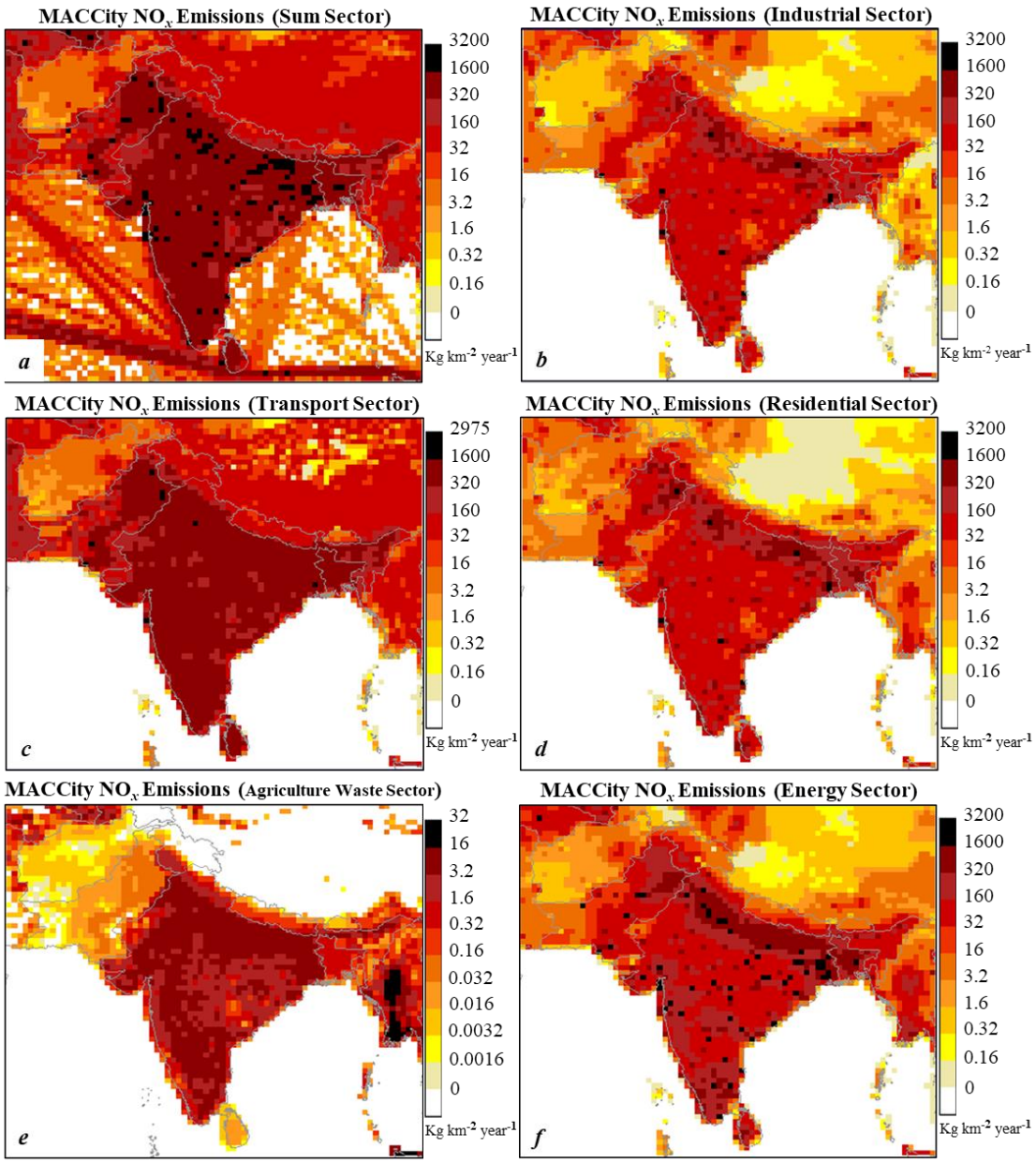


***Figure 4.*** *MACCity based average anthropogenic $NO_x$ emissions (kg $km^{-2}$ $year^{-1}$) from (a) sum sector (b) industrial sector (c) transport sector (d) residential sector (e) agricultural waste sector and (f) energy sector over South Asia during 2005-2016*


http://www.aloki.hu ● ISSN 1589 1623 (Print) ● ISSN 1785 0037 (Online)
DOI: http://dx.doi.org/10.15666/aeer/1705_1098911015

***Table 3.*** *MACCity average anthropogenic emissions of $NO_x$ in (kg $km^{-2}$ $year^{-1}$), Percentage change, slope of the regression equation and coefficient of determination $R^2$ over South Asia from January 2005 to December 2016*

| Emission sectors | Average emissions kg $km^{-2}$ $year^{-1}$ (2005-2016) | % Change (2005-2016) | (Slope of regression equation); (Coefficient of determination *R2*) |
|---|---|---|---|
| Sum sector | 2291691 | 42.7 | (73255.4 ± 2178.8); (0.99) |
| Agricultural waste sector | 8357 | 5.5 | (40.6 ± 12.6); (0.51) |
| Energy sector | 697934 | 35.3 | (19055.9 ± 1512.2); (0.94) |
| Industrial sector | 231386 | 20.7 | (3950.3 ± 213.9); (0.97) |
| Residential sector | 239234 | 12.9 | (2648.7 ± 177.9); (0.96) |
| Transportation sector | 816925 | 95.6 | (48034.7 ± 2017.3); (0.98) |

## *Zonal analyses of HCHO columns*

Data products from OMI sensor, for HCHO and $NO_2$ have been analyzed for spatiotemporal analysis of the tropospheric columns of HCHO and $NO_2$. Annual means values for both the gases, regression trends and percentage changes for the entire study period of 2005-2016, for South Asia and seven study zones are shown in *Table 4*.

***Table 4.*** *Summary of annual mean OMI-HCHO (× $10^{15}$ molecules $cm^{-2}$) and OMI-$NO_2$ (× $10^{15}$ molecules $cm^{-2}$), parameters of linear regression analysis and percentage change over entire South Asia and seven study zones during the period of 2005-2016*

| HCHO | Annual mean OMI-HCHO (× $10^{15}$ molec $cm^{-2}$) | Slope of regression equation | Coefficient of determination ($R^2$) | % Change |
|---|---|---|---|---|
| Zone-1 | 04.22 ± 0.05 | 0.004 ± 0.015 | 0.081 | 01.15 |
| Zone-2 | 10.12 ± 0.21 | 0.074 ± 0.03 | 0.45 | 08.34 |
| Zone-3 | 10.08 ± 0.13 | 0.091 ± 0.03 | 0.49 | 10.50 |
| Zone-4 | 10.20 ± 0.16 | 0.073 ± 0.04 | 0.29 | 08.22 |
| Zone-5 | 08.12 ± 0.14 | 0.080 ± 0.03 | 0.41 | 11.50 |
| Zone-6 | 09.88 ± 0.12 | 0.066 ± 0.05 | 0.16 | 07.58 |
| Zone-7 | 08.50 ± 0.12 | 0.081 ± 0.03 | 0.49 | 11.09 |
| South Asia | 06.22 ± 0.14 | 0.050 ± 0.01 | 0.53 | 09.86 |
| **$NO_2$** | **Annual mean OMI-HCHO (× $10^{15}$ molec $cm^{-2}$)** | **Slope of regression equation** | **Coefficient of determination ($R^2$)** | **% Change** |
| Zone-1 | 0.77 ± 0.01 | 0.004 ± 0.002 | 0.27 | 6.61 |
| Zone-2 | 2.43 ± 0.15 | 0.038 ± 0.009 | 0.67 | 18.91 |
| Zone-3 | 1.91 ± 0.06 | 0.020 ± 0.003 | 0.85 | 12.11 |
| Zone-4 | 1.82 ± 0.14 | 0.035 ± 0.006 | 0.76 | 23.64 |
| Zone-5 | 0.93 ± 0.02 | -0.005 ± 0.006 | 0.06 | -5.87 |
| Zone-6 | 1.81 ± 0.17 | 0.040 ± 0.006 | 0.81 | 27.96 |
| Zone-7 | 1.32 ± 0.04 | 0.009 ± 0.006 | 0.21 | 7.66 |
| South Asia | 0.83 ± 0.05 | 0.006 ± 0.003 | 0.34 | 7.89 |


http://www.aloki.hu ● ISSN 1589 1623 (Print) ● ISSN 1785 0037 (Online)
DOI: http://dx.doi.org/10.15666/aeer/1705_1098911015

From *Table 4*, it is clear that the highest annual average value for tropospheric HCHO column, averaged for the entire study period of 12 years has been observed for zone-4, as $(10.20 \pm 0.16) \times 10^{15}$ molecules $cm^{-2}$. While, the lowest value $(4.22 \pm 0.05) \times 10^{15}$ molecules $cm^{-2}$ for zone-1. The largest positive trend or change ($\Delta$HCHO = 11.50%) has been observed for zone-5, while the lowest trend of change ($\Delta$HCHO = 1.15) has been found for zone-1. This high value of change of HCHO column observed in zone-5, mainly representing the Myanmar region, can be attributed to the high rate of oil palms plantations in southern parts of Myanmar in the last decade. Oil palms have been reported to have a much stronger isoprene emission capacity (Lathière et al., 2010) than the tropical forests of South Asia (Stavrakou et al., 2014). With this plantation activity, associated changes to the landcovers and anthropogenic emissions due to urbanization and changing of natural vegetation with forest plantations have been reported to have significant impacts on the emissions of isoprene (Wiedinmyer et al., 2006) and isoprene being a linchpin for the connection between the satellite observations of tropospheric HCHO column and forested landcover (Wolf et al., 2016). Another high percentage of change in HCHO column, i.e. ($\Delta$HCHO = 11.09%) is observed in zone-7, comprising of the major forest cover on southwestern coast of Indian state Kerala and this region is characterized as a region, where the isoprene has been observed to have the longest lifetime in air (Surl et al., 2018) which also contributes to the high concentrations observed for HCHO column using OMI data. Because of capturing data in early afternoon at 13:40 local time, providing ample time for this longest living isoprene to get converted into HCHO.

Zone-3 also exhibits a considerable change ($\Delta$HCHO = 10.50%) over the study period. Emissions in this study zone are presented with compound influences, i.e., biogenic emissions from forested landcover regions of the states of Uttar Pradesh and Bihar in India and contributions from Nepalis forests. HCHO emissions in this zone are also contributed by the anthropogenic emissions from coal powered thermal electricity generation plants in the states of Uttar Pradesh and Bihar and cities of Jaipur and Lucknow and from the city of Katmandu from neighbouring Nepal. The weak positive trend found in zone-1 with ($\Delta$HCHO = 1.15%) over the span of 12 years can be attributed to the arid and dry landcover, presented mostly by desert landcover, barren rocks and dry sandy soils with weak biogenic sources available for HCHO emissions and the being the least populated region of South Asia, comprising of Baluchistan province of Pakistan and parts of Southwestern Afghanistan for any considerable or noticeable anthropogenic emissions.

Among rest of the zones, i.e. zone-2 with ($\Delta$HCHO = 8.34%) and zone-4 with ($\Delta$HCHO = 8.22%), primarily represent the zones of high anthropogenic emissions through the megacities of Lahore, Faisalabad and Delhi in zone-2, while, Dhaka and Kolkata in zone-4. In zone-2, Pyrogenic emissions contribution comes through crop residue burning activity in the plains of irrigated belts of Punjab, on both, Indian and Pakistani sides. In zone-4, the HCHO contribution is very compound in nature, as all the three, anthropogenic, pyrogenic and biogenic sources are contributing, especially for Bangladesh. Here, contribution to the emissions through pyrogenic sources come from the crop residue burning. While, mangroves of Sundarbans emit significant amounts of isoprene which according to a study, is one of the main biogenic VOC (Barr et al., 2003; Exton et al., 2015) and is a precursor of HCHO. Emissions from zone-6 with ($\Delta$HCHO = 7.58%) represents the regions of Indian states of Orissa and Chhattisgarh, marked with presence of extensive mining and coal powered electricity generation


http://www.aloki.hu ● ISSN 1589 1623 (Print) ● ISSN 1785 0037 (Online)
DOI: http://dx.doi.org/10.15666/aeer/1705_1098911015

power plants and therefore, high emissions through anthropogenic activities. This region is attributed for being the largest coal mining area, along with mega coal powered electricity production plants in eastern India. Mean annual change for South Asia for the study period 2005-2016, ($\Delta$HCHO = 9.86%) can be understood well with distinct anthropogenic, biogenic and selective pyrogenic sources of emissions of HCHO for different zones of land-use/landcover, contributing to the specific emissions of the tropospheric HCHO column.

### *Zonal analyses of $NO_2$ columns*

Annual means values of tropospheric $NO_2$ column, regression trends and percentage changes for the entire study period of 2005-2016, for South Asia and seven study zones are shown in *Table 4.* From *Table 4* tropospheric column of $NO_2$ for the study period 2005-2016 has been observed with the highest average annual value of $(2.43 \pm 0.15) \times 10^{15}$ molecules $cm^{-2}$ for zone-2, while the lowest value $(0.77 \pm 0.01) \times 10^{15}$ molecules $cm^{-2}$ is observed for zone-1. Emissions captured through OMI sensor of vertical column of $NO_2$ exhibits the largest positive trend of change with ($\Delta NO_2$ = 27.96%) in zone-6, and the lowest negative trend of change has been observed for zone-5 being ($\Delta NO_2$ = -5.87%). It is also interesting to note here, that the annual mean value for the entire study period for zone-5 being $(0.93 \pm 0.02) \times 10^{15}$ molecules $cm^{-2}$ is higher than the annual mean value observed in zone-1 $(0.77 \pm 0.01) \times 10^{15}$ molecules $cm^{-2,}$ but still the overall change for the entire study period of 12 years for zone-5 is less than zone-1. The largest trend of change found in zone-6 can be attributed to the Eastern coal mining zone of Indian states of Chhattisgarh and Orissa, where emissions of $NO_2$ have increased to 50 ± 20% from 2005-2015 (Krotkov et al., 2016) and are further complemented by 16 coal fired electricity power plants with a capacity of ~18000 Mega Watts (MW) and ~330 tons of NO*x* emissions annually (Sarath and Puja, 2014).

Zone-2 with a changing trend of ($\Delta NO_2$ = 18.91%) is characterized with anthropogenic emissions from thickly populated megacities of Delhi, and Lahore, the Industrial city of Faisalabad and also due to pyrogenic emissions from the biomass burning, which also increase the aerosol loading in the region, especially in post-monsoon and winter season (Tariq et al., 2015) from Indian and Pakistani Punjab region. This high aerosol loading may also result in underestimation of $NO_2$ due to shielding effect of aerosols such as PM2.5 (Jamstec, 2014). Increasing trend in this zone of (~1.58% rise per year) has been found closely consistent with the (Ghude et al., 2009) as of (1.76 ± 1.1% per year) for the South Asian countries. This zone-2 has also been found with the highest annual mean concentrations of column of $NO_2$ value for the entire study period of 2005-2016, i.e. $(2.43 \pm 0.15) \times 10^{15}$ molecules $cm^{-2}$ because of high anthropogenic activity due to rapid urbanization, increasing vehicular activity, more food requirement, high crop residue burning and high biofuel burning for heating purposes. (Azad and Kitada, 1998; Ghose et al., 2004; Badarinath et al., 2006, 2009; Ghude et al., 2008, 2009; Gurjar et al., 2008; Renuka et al., 2014; Ali et al., 2014; ul-Haq et al., 2014; Tariq and Ali, 2015; Tariq et al., 2016). Lowest Observed negative trend ($\Delta NO_2$ = -5.87%) has been found in zone-5, with annual mean value $(0.93 \pm 0.02) \times 10^{15}$ molecules $cm^{-2}$, with a consistently decreasing trend after the year 2011, reversing the positively changing trend observed till 2011 to a negative or decreasing trend for zone-5. Data from annual mean values for the vertical column of $NO_2$ reveal that this negative trend is consistent with the overall South Asian trends observed after the year 2011 to 2016 having ($\Delta NO_2$ = -5.29% making it ~-1.05% per year). Similar


http://www.aloki.hu ● ISSN 1589 1623 (Print) ● ISSN 1785 0037 (Online)
DOI: http://dx.doi.org/10.15666/aeer/1705_1098911015

declining trends have also been observed over China in studies by (Richter et al., 2015; Irie et al., 2016).

Zone-4 has also been observed as one of the positively trending regions with ($\Delta NO_2$ = 23.64%) and annual mean emissions of $NO_2$ for the entire study period to be $(1.82 \pm 0.14) \times 10^{15}$ molecules $cm^{-2}$. This region is attributed with high emissions of $NO_2$ due to anthropogenic activities from megacities of Kolkata and Dhaka and crop residue burning, especially in pre-monsoon seasons (ul-Haq et al., 2015). Zone-3 has also been reported with high amounts of annual mean $NO_2$ emissions for the study period, being $(1.91 \pm 0.06) \times 10^{15}$ molecules $cm^{-2}$ representing the changing trend to be ($\Delta NO_2$ = 12.11%). This region also contributes significantly enough for emissions of $NO_2$, due to its industrial and anthropogenic activities for having coal mining region and coal-powered electricity generation power plants in the states of Bihar and Uttar Pradesh, emissions from the Indian cities of Jaipur and Lucknow and from neighbouring city of Kathmandu in Nepal. Zone-7 exhibits the similar trend as discussed particularly for zone-5 and generally matches with the changing trends for South Asia. In this zone, a decreasing trend has also been seen for the annual mean values of $NO_2$ after 2011 up to 2016. This makes the overall spatial average emissions of $NO_2$ for the study period to be $(1.32 \pm 0.04) \times 10^{15}$ molecules $cm^{-2}$, with an overall changing trend as ($\Delta NO_2$ = 7.66%), and is more closely related to what was reported by (Ghude et al., 2008). South Asian mean annual change over the study period 2005-2016, ($\Delta NO_2$ = 7.89%) can be understood well with distinct anthropogenic, biogenic and pyrogenic sources of emissions of $NO_2$ for different zones of land-use/landcover, contributing and affecting to the specific emissions of the tropospheric $NO_2$ column.

### *Spatial distributions of HCHO and $NO_2$ columns*

Mean Spatial distributions derived from the annual mean values of OMI data for tropospheric columns of HCHO and $NO_2$ emissions along with the changing trends over South Asia for the entire study period, from 2005 to 2016 are shown in *Figure 5*.

In *row (a), Figure 5*, Spatial distributions of annual-mean area averaged tropospheric HCHO column ($\times 10^{15}$ molecules $cm^{-2}$), and annual-mean area averaged tropospheric $NO_2$ column ($\times 10^{15}$ molecules $cm^{-2}$) over South Asia for the study period of 2005 to 2016 are presented, retrieved through OMI data on left and middle columns respectively. Trends of these area averaged annual mean values, both for, HCHO and $NO_2$ from 2005 to 2016 over South Asia are also presented in the right column of *row (a), Figure 5*. A linear regression on the annual mean values of $NO_2$ data shows an increasing trend, with annual increase of ~0.66% and an overall increase of ~7.9% for the entire study period, with a slope of 0.006 (± 0.003), coefficient of determination ($R^2$ = 0.35) and *y*-intercept at 0.830426 (± 0.019072) $\times 10^{15}$ molecules $cm^{-2}$. These increasing trends of $NO_2$ for a period of first seven years from 2005-2011, with annual increase of ~1.86% making seven-year increase of ~13.01%, with a slope of 0.0172 ± 0.0029, coefficient of determination ($R^2$ = 0.88) and *y*-intercept at 0.7767 (± 0.013096) $\times 10^{15}$ molecules $cm^{-2}$ have been found well in agreement with the trends presented by (Ghude et al., 2009), i.e. 1.76 ± 1% per year over south Asia. However, $NO_2$ retrievals from OMI data, after reaching to a peak value in year 2011 with 0.845567 (± 0.040695) $\times 10^{15}$ molecules $cm^{-2}$ show consistently a negative change, till 2016. This decreasing trend has been observed for every two consecutive succeeding years for tropospheric $NO_2$ columns, showing the consistency in this declining trend. In the last five years of the study, from 2012 to 2016, the rate of change per year has been


http://www.aloki.hu ● ISSN 1589 1623 (Print) ● ISSN 1785 0037 (Online)
DOI: http://dx.doi.org/10.15666/aeer/1705_1098911015

observed to be reduced with decreasing values of $NO_2$ column, having an annual decrease of ~1.06% as compared to the value of change for the first seven years of the study. i.e. ~1.86%, and making an overall decrease for the last five years of ~5.29%, with a slope of -0.012 (± 0.007), coefficient of determination ($R^2$ = 0.50) and *y*-intercept at 0.907322 (± 0.023287) $\times 10^{15}$ molecules $cm^{-2}$. Similar decreasing trends of the tropospheric $NO_2$ column have also been reported in China after the year 2011, where this rate of decline has been reported to be ~6% $year^{-1}$(Richter et al., 2015; Irie et al., 2016). Reasons for lowering the values of the tropospheric column of $NO_2$ could be linked to the shift in meteorological regions, affecting. e.g., the rates of chemical reactions and air mass visibility for satellite observations in troposphere (Voulgarakis et al., 2010) and due to strategies adopted for lowering NOx emissions through technological improvements like adoption of cleaner technologies and also due to some decline in the economic activity related to NOx emissions (Hilboll et al., 2017).

Linear regression analysis performed on the area averaged annual mean values of HCHO data shows an increasing trend over South Asia, with an annual increase of ~0.74% and an overall increase of ~9.86% for the study period of twelve years, with a slope of 0.050508 (± 0.014932), coefficient of determination ($R^2$ = 0.53) and *y*-intercept at 6.220404 (± 0.109894) $\times 10^{15}$ molecules $cm^{-2}$. Such increasing trends of HCHO over countries of South Asia have also been reported in the study by (De Smedt et al., 2010). These increasing trends for HCHO emissions could also be associated with the increasing anthropogenic sources of emission in South Asia as shown by the results from the MACCity emission data sources, which indicate that for the period of 2005-2016 anthropogenic emissions have been increased to about 22% and hence the overall increase in HCHO emissions.

In *Figure 5*, *rows (b), (c), (d)* and *(e)* also represent spatial distributions of area averaged seasonal mean values of HCHO and $NO_2$ columns averaged from OMI monthly mean data for the entire study period of 12 years from 2005 to 2016 for Pre-Monsoon, Monsoon, Post-Monsoon and Winter seasons respectively. Seasonal spatial distributions of HCHO and $NO_2$ columns show the variations of emissions with the changing seasonal conditions over different landuse/landcovers. In *Figure 5*, *row (b)*, HCHO column exhibits higher concentrations for pre-monsoon season, observed along the Indo-Gangetic Basin (IGB) with the forest cover, especially along the foothills of the Himalayas in northwestern India, industrial landuse and activity in the Eastern mining zone of India, biogenic emissions from the mangrove forests (Barr et al., 2003; Exton et al., 2015; Sippo et al., 2016) of Sundarbans in Bangladesh and the forest cover of western Ghats in the states of Kerala and around. Similar anthropogenic and biogenic emissions have also been observed from Myanmar. In *Figure 5*, *row (b)*, the spatial distribution of tropospheric $NO_2$ column for pre-monsoon season retrieved through OMI also highlights the megacities of Lahore and Delhi representing the major contributions through anthropogenic emissions and from crop residue and biomass burning for heating purposes. These pre-monsoon, spring seasonal high values may be associated with the meteorological conditions as well (ul-Haq et al., 2015). Such highlighted emissions are also observed in the in the Eastern mining zone of India in the states of Chhattisgarh and Orissa, also the pre-monsoon pyrogenic emissions are also highlighted in the Bangladesh region.


http://www.aloki.hu ● ISSN 1589 1623 (Print) ● ISSN 1785 0037 (Online)
DOI: http://dx.doi.org/10.15666/aeer/1705_1098911015

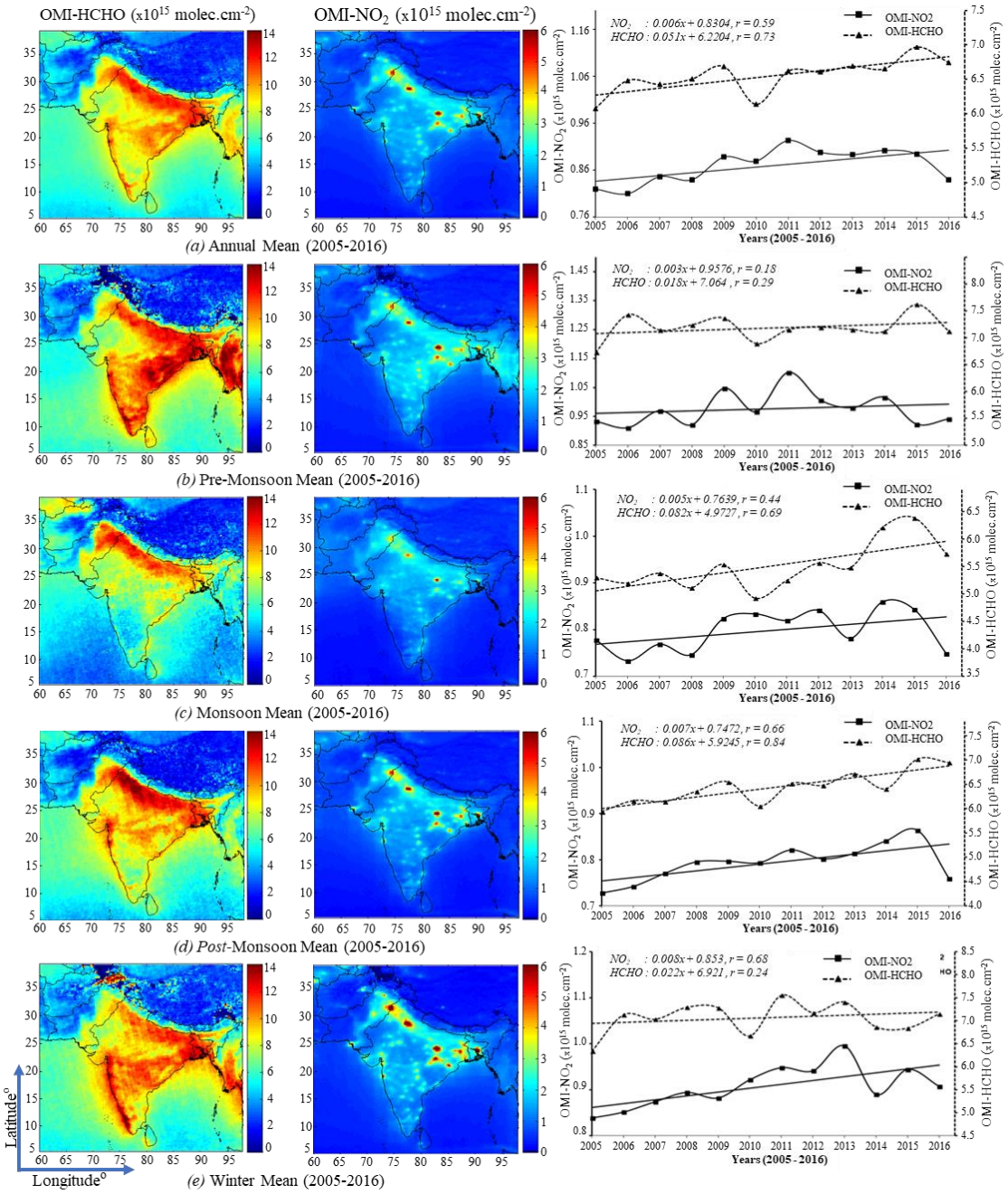


***Figure 5.*** *Annual mean area averaged spatial distributions of tropospheric columns of HCHO and $NO_2$ (× $10^{15}$ molecules $cm^{-2}$) over South Asia for study period of (2005-2016) along with the varying trend for 12 years is shown in row (a), in left and middle columns respectively. Seasonal, mean area averaged spatial distributions of HCHO and $NO_2$ columns (× $10^{15}$ molecules $cm^{-2}$) along with the varying seasonal trend for entire study period for all the four seasons over South Asia from (2005-2016) are shown as, Pre-Monsoon in row (b), monsoon in row (c), post-monsoon in row (d) and winter in row (e), respectively*

Spatial distribution of HCHO and $NO_2$ columns for the monsoon season (*Fig. 5*, *row c*), exhibits relatively low activity for both $NO_2$ and HCHO emissions for the underlying landcovers. Lower values of HCHO column in the monsoon conditions could be


http://www.aloki.hu ● ISSN 1589 1623 (Print) ● ISSN 1785 0037 (Online)
DOI: http://dx.doi.org/10.15666/aeer/1705_1098911015

ascribed to low wind speeds, high humidity and rain driven washout of the gaseous air pollutants (Verma et al., 2015). This can also be seen from *Figure 2*, where low wind vectors are observed in monsoon season along with high precipitation resulting in this kind of washout phenomenon of pollutants. Whereas, these seasonal low values observed for $NO_2$ could be associated with the higher concentration of (Hydroxyl) OH ions, making an increased activity of photo-dissociation of $NO_2$, advection of clean air mass and due to increased solar radiation for having longer day hours (Ravindra et al., 2003; Ghude et al., 2009; Yoo et al., 2014).

Spatial distribution of HCHO column over South Asia for post monsoon season (*Fig. 5, row d*), shows lower concentrations and that can be associated with low biogenic emissions especially from the forested regions due to leaf phenological variations depicted by the low values of NDVI $0.379 \pm 0.029$, derived by MODIS onboard Terra satellite , as compared to pre-monsoon season with NDVI values to be $0.527 \pm 0.018$, for the months of March, April and May. These phenological changes in post monsoon season could be one of the reasons for lower values of isoprene emissions and hence the lower concentrations of HCHO column observations (Surl et al., 2018). Post-monsoon relatively higher concentrations of $NO_2$ column are observed due to the activity of large-scale crop waste burning (ul-Haq et al., 2014).

Spatial distribution of HCHO column over South Asia for winter season (*Fig. 5, row 5*) shows lower concentrations of HCHO, as compared to the summer season. These relatively low emissions may be connected to the lower emissions of Isoprene in winters, as the Isoprene emissions have a clear distinct seasonal cycle, showing high emissions in the summers than in winters (Malik et al., 2018). And as this isoprene is oxidized with air, it gets converted to HCHO (Palmer et al., 2003, 2006), therefore the two associated low emissions could be linked in the winter season. High emissions have been observed for $NO_2$ in the winter season due to more crop residue burning in the winters in the region of Indian and Pakistani Punjab, especially highlighting the regions near Lahore, and Delhi around, two mega cities with anthropogenic emissions as well. Also, the higher concentrations have been found in the eastern mining zones of India and emissions from the Bangladesh side.

## Conclusion

In this study a spatiotemporal assessment of two important atmospheric air pollutants, i.e. HCHO and $NO_2$ has been carried out over South Asia, being the most thickly populated region of the world, by using satellite remote sensing data from OMI sensor onboard Aura satellite. This study spans over a period of 12 years, from 2005 to 2016. Different analysis on the remote sensing data for these gases, help in identifying three distinct types of sources of emissions for these atmospheric pollutants, i.e. emissions through anthropogenic activities, emissions through pyrogenic activities and emissions through nature or biogenic sources. Further, these three distinct sources have very specific associations with the different landuse/landcovers. These associations are explained and analyzed in seven different study zones, selected at different geographical locations of South Asia, representing different landuse/landcovers ranging from the arid desert like areas, to thickly populated areas, to mountainous forested landcovers, to the mangroves forest cover, to the mining regions and to the agricultural belts defining the main landcovers of the region. Analyses of the annual spatial data for both the gases for a period from 2005 to 2016 show an overall increasing trend for anthropogenic $NO_2$


http://www.aloki.hu ● ISSN 1589 1623 (Print) ● ISSN 1785 0037 (Online)
DOI: http://dx.doi.org/10.15666/aeer/1705_1098911015

emissions. A linear regression on the annual mean values of $NO_2$ data shows this trend with annual increase of ~0.66% and an overall increase of ~7.9% for the entire study period, with a slope of 0.006 (± 0.003), coefficient of determination ($R^2$ = 0.35) and *y*-intercept at 0.830426 (± 0.019072) $\times 10^{15}$ molecules $cm^{-2}$. An important finding in this trend analysis is that for the first seven years of the study, i.e. from 2005 to 2011, $NO_2$ emissions are increasing with a faster rate of about ~1.86% per year but in the last six years, i.e. from 2012 to 2016 this rate has been observed to be reduced to ~1.06% annually, making this rising trend to check. Reasons for lowering the values of the tropospheric column of $NO_2$ could be linked to the shift in meteorological regions, affecting, e.g., the rates of chemical reactions and air mass visibility for satellite observations in troposphere, and due to strategies adopted for lowering $NO_x$ emissions through technological improvements like adoption of cleaner technologies and also due to some decline in the economic activity related to NOx emissions. Similar increasing trends have been observed for HCHO emissions for South Asia. Linear regression analysis performed on the area averaged annual mean values of HCHO data shows this increasing trend over South Asia, with annual increase of ~0.74% and an overall increase of ~9.86% for the study period of 12 years, with a slope of 0.050508 (± 0.014932), coefficient of determination ($R^2$ = 0.53) and *y*-intercept at 6.220404 (± 0.109894) $\times 10^{15}$ molecules $cm^{-2}$. These increasing trends for HCHO emissions could also be associated with the increasing anthropogenic sources of emission in South Asia as shown by the results from the MACCity emission data sources, which indicate that, for the period of 2005-2016 anthropogenic emissions have been increased to about 22% and hence the overall increase in HCHO emissions. Seasonality has been observed in the emission trends of HCHO and $NO_2$ over South Asia as, the effects of seasonal changes are associated sometimes with anthropogenic activities and sometimes with the biogenic and pyrogenic activities, resulting the corresponding impacts on the emissions of these gases in atmosphere. For further localized analysis, seven study zones have been analyzed, representing some of the available representative variations of landuse and landcovers. These zones have been typically observed in the context of anthropogenic, natural or biogenic and pyrogenic sources of emissions.

## REFERENCES

[1] Ali, M., Tariq, S., Mahmood, K., Daud, A., Batool, A., ul-Haq, Z. (2014): A study of aerosol properties over Lahore (Pakistan) by using AERONET data. – Asia-Pacific J Atmos Sci 50: 153-162.

[2] Amnuaylojaroen, T., Barth, M. C., Emmons, L. K., Carmichael, G. R., Kreasuwun, J., Prasitwattanaseree, S., Chantara, S. (2014): Effect of different emission inventories on modeled ozone and carbon monoxide in Southeast Asia. – Atmos. Chem. Phys. 14: 12983-13012. http://dx. doi.org/10.5194/acp-14-12983-2014.

[3] Azad, A. K., Kitada, T. (1998): Characteristics of the air pollution in the city of Dhaka, Bangladesh in winter. – Atmos Environ 32(11): 1991-2005.

[4] Badarinath, K. V. S., Chand, K. T. R., Prasad, K. V. (2006): Agriculture crop residue burning in the Indo-Gangetic Plains—a study using IRSP6 AWiFS satellite data. – Curr Sci 91: 1085-1089.

[5] Badarinath, K. V. S., Kharol, S. K., Sharma, A. R., Prasad, V. K. (2009): Analysis of aerosol and carbon monoxide characteristics over Arabian Sea during crop residue burning period in the Indo-Gangetic Plains using multi-satellite remote sensing datasets. – J Atmos Solar Terr Phys 71: 1267-1276.


http://www.aloki.hu ● ISSN 1589 1623 (Print) ● ISSN 1785 0037 (Online)
DOI: http://dx.doi.org/10.15666/aeer/1705_1098911015

[6] Barck, C., Lundahl, J., Halldén, G., Bylin, G. (2005): Brief exposures to $NO_2$ augment the allergic inflammation in asthmatics. – Environmental Research 97: 58-66.

[7] Barkley, M. P., Palmer, P. I., Kuhn, U., Kesselmeier, J., Chance, K., Kurosu, T. P., Martin, R. V., Helmig, D., Guenther, A. (2008): Net ecosystem fluxes of isoprene over tropical South America inferred from Global Ozone Monitoring Experiment (GOME) observations of HCHO columns. – J. Geophys. Res.-Atmos. 113: d20304. https://doi.org/10.1029/2008JD009863.

[8] Barkley, M. P., Smedt, I. D., Van Roozendael, M., Kurosu, T. P., Chance, K., Arneth, A., Hagberg, D., Guenther, A., Paulot, F., Marais, E. (2013): Top-down isoprene emissions over tropical south America inferred from SCIAMACHY and OMI formaldehyde columns. – J Geophys Res Atmos 118(12): 6849-6868. https://doi.org/10.1002/jgrd.50552.

[9] Barr, J. G. J. D., Fuentes, N., Wang, Y., Edmonds, J. C., Zieman, B. P., Hayden, D. L., Childers. (2003): Red mangroves emit hydrocarbons. – Southeast. Nat. 2: 499-510.

[10] Bauwens, M. T., Stavrakou, J. F., Müller, I., De Smedt, M., Van Roozendael, G. R., van der Werf, C., Wiedinmyer, J. W., Kaiser, K., Sindelarova, Guenther, A. (2016): Nine years of global hydrocarbon emissions based on source inversion of OMI formaldehyde observations. – Atmos. Chem. Phys. 16: 10,133-10,158. DOI: 10.5194/acp-16-10133-2016.

[11] Boersma, F., Bucsela, E., Brinksma, E., Gleason, J. F. (2002): $NO_2$. – In: Chance, K. (ed.) OMI Algorithm Theoretical Basis Document. OMI Trace Gas Algorithms. – Smithsonian Astrophysical Observatory, Cambridge, Vol. IV, pp 13-36.

[12] Boersma, K. F., Eskes, H. J., Brinksma, E. J. (2004): Error analysis for tropospheric $NO_2$ retrieval from space. – J Geophys Res Atmos 109(D4).

[13] Boersma, K. F., Jacob, D. J., Bucsela, E. J., Perring, A. E., Dirksen, R., Yantosca, R. M., Cohen, R. C. (2008): Validation of OMI tropospheric $NO_2$ observations during INTEX-B and application to constrain NOx emissions over the eastern United States and Mexico. – Atmos Environ 42(19): 4480-4497.

[14] Boersma, K. F., Jacob, D. J., Trainic, M., Rudich, Y., De Smedt, I., Dirksen, R., Eskes, H. J. (2009): Validation of urban $NO_2$ concentrations and their diurnal and seasonal variations observed from the SCIAMACHY and OMI sensors using in situ surface measurements in Israeli cities. – Atmos Chem Phys 9: 3867-3879. DOI: 10. 5194/acp-9-3867-2009.

[15] Boersma, K. F., Eskes, H. J., Dirksen, R. J., van der A, R. J., Veefkind, J. P., Stammes, P., Huijnen, V., Kleipool, Q. L., Sneep, M., Claas, J., Leitao, J., Richter, A., Zhou, Y., Brunner, D. (2011): An improved tropospheric $NO_2$ column retrieval algorithm for the Ozone Monitoring Instrument. – Atmos Meas Tech 4: 1905-1928.

[16] Bucsela, E. J., Celarier, E. A., Wenig, M. O., Gleason, J. F., Veefkind, J. P., Boersma, K, F., Brinksma, E. J. (2006): Algorithm for $NO_2$ vertical column retrieval from the Ozone Monitoring Instrument. – IEEE Trans Geosci Remote Sens 44: 1245-1258.

[17] Case, G. D., Dixon, J. S., Schooley, J. C. (1979): Interactions of blood metalloproteins with nitrogen oxides and oxidant air pollutants. – Environmental Research 20: 43-65.

[18] Chance, K., Palmer, P. I., Spurr, R. J. D., Martin, R. V., Kurosu, T. P., Jacob, D. J. (2000): Satellite observations of formaldehyde over North America from GOME. – Geophys. Res. Lett. 27: 3461-3464. DOI: 10.1029/2000GL011857.

[19] Curci, G., Palmer, P. I., Kurosu, T. P., Chance, K., Visconti, G. (2010): Estimating European volatile organic compound emissions using satellite observations of formaldehyde from the Ozone Monitoring Instrument. – Atmos. Chem. Phys. 10: 11501-11517. https://doi.org/10.5194/acp-10-11501-2010.

[20] De Graaf, M., Sihler, H., Tilstra, L. G., Stammes, P. (2016): How big is an OMI pixel? – Atmos. Meas. Tech. 9: 3607-3618. DOI: 10.5194/amt-9- 3607-2016.

[21] De Smedt, I., Müller, J. F., Stavrakou, T., van der A, R., Eskes, H., Van Roozendael, M. (2008): Twelve years of global observations of formaldehyde in the troposphere using


http://www.aloki.hu ● ISSN 1589 1623 (Print) ● ISSN 1785 0037 (Online)
DOI: http://dx.doi.org/10.15666/aeer/1705_1098911015

GOME and SCIAMACHY sensors. – Atmos. Chem. Phys. 8: 4947-4963. DOI: 10.5194/acp-8-4947-2008.

[22] De Smedt, T., Stavrakou, J.-F., Müller, R. J., van der, A., Roozendael, M. V. (2010): Trend detection in satellite observations of formaldehyde tropospheric columns. – Geophysical Research Letters 37: L18808. DOI: 10.1029/2010GL044245.

[23] De Smedt, I., Stavrakou, T., Hendrick, F., Danckaert, T., Vlemmix, T., Pinardi, G., Theys, N., Lerot, C., Gielen, C., Vigouroux, C., et al. (2015): Diurnal, seasonal and long-term variations of global formaldehyde columns inferred from combined OMI and GOME-2 observations. – Atmos. Chem. Phys 15: 12,519-12,545. DOI: 10.5194/acp-15-12519-2015.

[24] Diehl, T., Heil, A., Chin, M., Pan, X., Streets, D., Schultz, M., Kinne, S. (2012): Anthropogenic, biomass burning, and volcanic emissions of black carbon, organic carbon, and SO2 from 1980 to 2010 for hindcast model experiments. – Atmos. Chem. Phys. Discuss. 12: 24895-24954. http://dx.doi.org/10.5194/acpd-12-24895-2012.

[25] Dobber, M. R., Dirksen, R. J., Levelt, P. F., van den Oord, G. H. J., Voors, R. H. M., Kleipool, Q., Jaross, G., Kowalewski, M., Hilsenrath, E., Leppelmeier, G. W., de Vries, J., Dierrsen, W., Rozemeijer, N. C. (2006): Ozone Monitoring Instrument calibration. – IEEE Trans. Geosci. Remote Sens. 44: 1209. DOI: 10.1109/TGRS.2006.869987.

[26] Exton, D. A., McGenity, T. J., Steinke, M., Smith, D. J. Suggett, D. J. (2015): Uncovering the volatile nature of tropical coastal marine ecosystems in a changing world. – Glob. Change Biol. 21: 1383-1394. DOI: 10.1111/gcb.12764.

[27] Fu, T.-M., Jacob, D. J., Palmer, P. I., Chance, K., Wang, Y. X., Barletta, B., Blake, D. R., Stanton, J. C., Pilling, M. J. (2007): Space-based formaldehyde measurements as constraints on volatile organic compound emissions in east and south Asia and implications for ozone. – J. Geophys. Res. 112: D06312. DOI: 10.1029/2006JD007853.

[28] Ghose, M. K., Paul, R., Banerjee, S. K. (2004): Assessment of the impacts of vehicular emissions on urban air quality and its management in Indian context: the case of Kolkata (Calcutta). – Environ Sci Policy 7: 345-351.

[29] Ghude, S. D., Fadnavis, S., Beig, G., Polade, S. D., van der A, R. J. (2008): Detection of surface emission hot spots, trends, and seasonal cycle from satellite-retrieved $NO_2$ over India. – J Geophys Res Atmos 113. DOI: 10.1029/2007JD009615.

[30] Ghude, S. D., Van der A, R. J., Beig, G., Fadnavis, S., Polade, S. D. (2009): Satellite derived trends in $NO_2$ over the major global hotspot regions during the past decade and their intercomparison. – Environ Pollut 157: 1873-1878.

[31] Gonzi, S., Palmer, P. I., Barkley, M. P., De Smedt, I., Van Roozendael, M. (2011): Biomass burning emission estimates inferred from satellite column measurements of HCHO: Sensitivity to co-emitted aerosol and injection height. – Geophys. Res. Lett. 38: L14807. DOI: 10.1029/ 2011GL047890.

[32] Granier, C., Bessagnet, B., Bond, T., D'Angiola, A., van der Gon, D. H., Frost, G. J., Heil, A., Kaiser, J. W., Kinne, S., Klimont, Z., Kloster, S., Lamarque, J.-F., Liousse, C., Masui, T., Meleux, F., Mieville, A., Ohara, T., Raut, J., Riahi, K., Schultz, M. G., Smith, S. J., Thompson, A., van Aardenne, J., van der Werf, G. R., van Vuuren, D. P. (2011): Evolution of anthropogenic and biomass burning emissions of air pollutants at global and regional scales during the 1980-2010 period. – Clim. Change 109 (1-2): 163-190. http://dx.doi.org/10.1007/s10584- 011-0154-1.

[33] Gurjar, B. R., Butler, T. M., Lawrence, M. G., Lelieveld, J. (2008): Evaluation of emissions and air quality in megacities. – Atmos Environ 42: 1593-1606.

[34] Hassan, S. K., El-Abssawy, A. A., Khoder, M. I. (2018): Effect of seasonal variation on the levels and behaviors of formaldehyde in the atmosphere of a suburban area in Cairo, Egypt. – Asian Journal of Atmospheric Environment 12(4): 356-368.

[35] Harrison, S. P., Morfopoulos, C., Dani, K. G. S., Prentice, I. C., Arneth, A., Atwell, B. J., Michael, P., Barkley, M. P., Leishman, M. R., Loreto, F., Belinda, E., Medlyn, B. E., Niinemets, U., Possell, M., Pe-uelas, J., Wright, I. J. (2013): Volatile isoprenoid


http://www.aloki.hu ● ISSN 1589 1623 (Print) ● ISSN 1785 0037 (Online)
DOI: http://dx.doi.org/10.15666/aeer/1705_1098911015

emissions from plastid to planet. – New Phytologist 197: 49-57. DOI: 10.1111/nph.12021.

[36] Hilboll, A., Richter, A., Burrows, J. P. (2017): $NO_2$ pollution over India observed from space — the impact of rapid economic growth, and a recent decline. – Atmos. Chem. Phys. Discuss. DOI: 10.5194/acp-2017-101: 2017.

[37] Irie, H., Muto, T., Itahashi, S., Kurokawa, J., Uno, I. (2016): Turnaround of tropospheric nitrogen dioxide pollution trends in China, Japan, and South Korea. – Sola 12: 170-174. DOI: 10.2151/sola.2016-035. 2016.

[38] JAMSTEC (2014): JAMSTEC 2014 Annual Report. – http://www.godac.jamstec.go.jp/catalog/data/doc_catalog/media/AR_2014_all.pdf (accessed on 17 May 2019).

[39] Joshi, R. M. (2015): Education in South Asia. – In: Smelser, N. J., Baltes, P. B. (eds.) International Encyclopedia of the Social & Behavioral Sciences, 2nd Ed.. Elsevier, Amsterdam, pp. 194-197.

[40] Kalnay, E., Kanamitsu, M., Kistler, R., Collins, W., Deaven, D., Gandin, L., Iredell, M., Saha, S., White, G., Woollen, J., Zhu, Y., Chelliah, M., Ebisuzaki, W., Higgins, W., Janowiak, J., Mo, K. C., Ropelewski, C., Wang, J., Leetmaa, A., Reynolds, R., Jenne, R., Joseph, D. (1996): The NCEP/NCAR 40-year reanalysis project. – Bull. Am. Meteorol. Soc. 77: 437-471.

[41] Kaczorowski, J., Perelli, A. (2004): Inversion of CO and $NO_x$ emissions using the adjoint of the IMAGES model. – Atmos. Chem. Phys. Discuss. 4: 7985-8068.

[42] Krotkov, N. A., McLinden, C. A., Li, C., Lamsal, L. N., Celarier, E. A., Marchenko, S. V., Swartz, W. H., Bucsela, E. J., Joiner, J., Duncan, B. N., Boersma, K. F., Veefkind, J. P., Levelt, P. F., Fioletov, V. E., Dickerson, R. R., He, H., Lu, Z., Streets, D. G. (2016): Aura OMI observations of regional $SO_2$ and $NO_2$ pollution changes from 2005 to 2015. – Atmos. Chem. Phys. 16: 4605-4629. https://doi.org/10.5194/acp-16-4605-2016.

[43] Kurosu, T. P. (2008): OMHCHO README FILE. – https://www.cfa.harvard.edu/atmosphere/Instruments/OMI/PGEReleases/READMEs/OMHCHO_README.pdf (accessed on 12 May 2019).

[44] Lamarque, J., Bond, T. C., Eyring, V., Granier, C., Heil, A., Klimont, Z., Lee, D., Liousse, C., Mieville, A., Owen, B., Schultz, M. G., Shindell, D., Smith, S. J., Stehfest, E., Van Aardenne, J., Cooper, O. R., Kainuma, M., Mahowald, N., McConnell, J. R., Naik, V., Riahi, K., van Vuuren, D. P. (2010): Historical (1850-2000) gridded anthropogenic and biomass burning emissions of reactive gases and aerosols: methodology and application. – Atmos. Chem. Phys. 10: 7017-7039. http://dx.doi.org/10.5194/acp-10-7017-2010.

[45] Lamsal, L. N., Martin, R. V., van Donkelaar, A., Celarier, E. A., Bucsela, E. J., Boersma, K. F., Dirksen, R., Luo, C., Wang, Y. (2010): Indirect validation of tropospheric nitrogen dioxide retrieved from the OMI satellite instrument: insight into the seasonal variation of nitrogen oxides at northern midlatitudes. – J Geophys Res 115: D05302. DOI: 10.1029/2009JD013351.

[46] Lathière, J., Hauglustaine, D. A., Friend, A. D., De Noblet-Ducoudré, N., Viovy, N., Folberth, G. A. (2006): Impact of climate variability and land use changes on global biogenic volatile organic compound emissions. – Atmos. Chem. Phys. 6: 2129-2146. https://doi.org/10.5194/acp-6-2129-2006.

[47] Lathière, J., Hewitt, C. N., Beerling, D. J. (2010): Sensitivity of isoprene emissions from the terrestrial biosphere to 20th century changes in atmospheric CO 2 concentration, climate, and land use. – Global Biogeochemical Cycles - Global Biogeochem Cycle 24. DOI: 10.1029/2009GB003548.

[48] Lee, Y.-N., Zhou, X., Kleinman, L. I., Nunnermacker, L. J. Springston, S., Daum, P., Newman, L., Keigley, W. G., Holdren, M. W., Spicer, C., Young, V., Fu, B., Parrish, D., Holloway, J., Williams, J., Roberts, J., Ryerson, T. B., Fehsenfeld, F. (1998): Atmospheric chemistry and distribution of formaldehyde and several multioxygenated


http://www.aloki.hu ● ISSN 1589 1623 (Print) ● ISSN 1785 0037 (Online)
DOI: http://dx.doi.org/10.15666/aeer/1705_1098911015

carbonyl compounds during the 1995 Nashville/Middle Tennessee Ozone Study – J. Geophys. Res. 103: 22,449-22,462.

[49] Levelt, P. F., Van den Oord, G. H. J., Dobber, M. R., Mälkki, A., Visser, H., De Vries, J., Stammes, P., Lundell, J. O. V., Saari, H. (2006): The Ozone Monitoring Instrument. – IEEE Transaction on Geoscience and Remote Sensing 44(5): 1093-1101.

[50] Malik, T. G., Gajbhiye, T., Pandey, S. K. (2018): Seasonality in emission patterns of isoprene from two dominant tree species of Central India: implications on terrestrial carbon emission and climate change. – Proceedings of the International Academy of Ecology and Environmental Sciences 8(4): 204-212.

[51] Marais, E. A., Jacob, D. J., Kurosu, T. P., Chance, K., Murphy, J. G., Reeves, C., Mills, G., Casadio, S., Millet, D. B., Barkley, M. P., Paulot, F., Mao, J. (2012): Isoprene emissions in Africa inferred from OMI observations of formaldehyde columns. – Atmos. Chem. Phys. 12: 6219-6235, https://doi.org/10.5194/acp-12-6219.

[52] Marais, E. A., Jacob, D. J., Wecht, K., Lerot, C., Zhang, L., Yu, K., Kurosu, T. P., Chance, K., Sauvage, B. (2014): Anthropogenic emissions in Nigeria and implications for ozone air quality: A view from space. – Atmos. Environ. 99: 32-40. DOI: 10.1016/j.atmosenv.2014.09.055.

[53] Maroziene, L., Grazuleviciene, R. (2002): Maternal exposure to low-level air pollution and pregnancy outcomes: a population-based study. – Environ Health 9: 1: 6.

[54] Millet, D. B., Jacob, D. J., Turquety, S., Hudman, C. R., Wu, S., Fried, A., James Walega, J., Heikes, B. G., Blake, D. R., Singh, H. B., Anderson, B. E., Clarke, A. D. (2006): Formaldehyde distribution over North America: Implications for satellite retrievals of formaldehyde columns and isoprene emission. – Journal of Geophysical Research 111: D24S02.

[55] Millet, D. B., Jacob, D. J., Boersma, K. F., Fu, T. M., Kurosu, T. P., Chance, K., Heald, C. L., Guenther, A. (2008): Spatial distribution of isoprene emissions from North America derived from formaldehyde column measurements by the OMI satellite sensor. – J. Geophys. Res. 113: D02307. DOI: 10.1029/2007JD008950.

[56] Nowlan, C. R., Liu, X., Janz, S. J., Kowalewski, M. G., Chance, K., Follette-Cook, M. B., Fried, A., González Abad, G., Herman, J. R., Judd, L. M., Kwon, H.-A., Loughner, C. P., Pickering, K. E., Richter, D., Spinei, E., Walega, J., Weibring, P., Weinheimer, A. J. (2018): Nitrogen dioxide and formaldehyde measurements from the GEOstationary Coastal and Air Pollution Events (GEO-CAPE) airborne simulator over Houston, Texas. – Atmos. Meas. Tech. 11: 5941-5964. https://doi.org/10.5194/amt-11-5941-2018.

[57] Palmer, P. I., Jacob, D. J., Chance, K. V., Martin, R. V. D. R. J., Kurosu, T. P., Bey, I., Yantosca, R. M., Fiore, A. M. (2001): Air mass factor formulation for spectroscopic measurements from satellites: Application to formaldehyde retrievals from the Global Ozone Monitoring Experiment. – J. Geophys. Res. 106: 14539- 14550. DOI: 10.1029/2000JD900772.

[58] Palmer, P. I., Jacob, D. J., Fiore, A. M., Martin, R. V., Chance, K., Kurosu, T. P. (2003): Mapping isoprene emissions over North America using formaldehyde column observations from space. – J. Geophys. Res.-Atmos. 108: 4180. https://doi.org/10.1029/2002JD002153. 2003.

[59] Palmer, P. I., Abbot, D. S., Fu, T.-M., Jacob, D. J., Chance, K., Kurosu, T. P., Guenther, A., Wiedinmyer, C., Stanton, J. C., Pilling, M. J., Pressley, S. N., Lamb, B., Sumner, A. L. (2006): Quantifying the seasonal and interannual variability of North American isoprene emissions using satellite observations of the formaldehyde column. – J. Geophys. Res.-Atmos. 111: D12315. https://doi.org/10.1029/2005JD006689. 2006.

[60] Parra, M. A., Elustondo, D., Bermejo, R., Santamaria, J. M. (2009): Ambient air levels of volatile organic compounds (VOC) and nitrogen dioxide ($NO_2$) in a medium size city in Northern Spain. – Science of the Total Environment 407: 999-1009.


http://www.aloki.hu ● ISSN 1589 1623 (Print) ● ISSN 1785 0037 (Online)
DOI: http://dx.doi.org/10.15666/aeer/1705_1098911015

[61] Ravindra, K., Mor S., Ameena, A., Kamyotra, J. S., Kaushik, C. P. (2003): Variation in spatial pattern of criteria air pollutants before and during initial rain of monsoon. – Environ Monit Assess 87: 145-153.
[62] Renuka, K., Gadhavi, H., Jayaraman, A., Lal, S.., Naja, M., Rao, S. V. B. (2014): Study of ozone and $NO_2$ over Gadanki—a rural site in South India. – J Atmos Chem 71: 95-112.
[63] Richter, A., Hilboll, A., Burrows, J. P. (2015): Revisiting satellite derived tropospheric $NO_2$ trends. – http://presentations.copernicus.org/EGU2015-10674_presentation.pdf.
[64] Sander, S. P., Finalyson-Pitts, B. J., Friedl, R. R., Golden, D. M., Huie, R. E., Keller-Rudeck, H., Kolb, C. E., Kurylo, M. J., Molina, M. J., Moortgat, G. K., Orkin, L. V., Ravishankara, A. R., Wine, P. H.(2006): Chemical Kinetics and Photochemical Data for Use in Atmospheric Studies. Evaluation number 15, NASA Panel for Data Evaluation. – JPM Publication 06-2, Jet Propulsion Laboratory, Pasadena.
[65] Sarath, K., Guttikunda, P. J. (2014): Atmospheric emissions and pollution from the coal-fired thermal power plants in India. – Atmospheric Environment 92: 449-460.
[66] Ghude, S. D., Van der A, R. J., Beig, S., Fadnavis, Polade, S. D. (2009): "Satellite derived trends in $NO_2$ over the major global hotspot regions during the past decade and their inter-comparison". – Environmental Pollution 157(6): 1873-1878.
[67] Seligman, D. (2008): World's Major Rivers. An Introduction to International Water Law with Case Studies. – Colorado River Commission of Nevada, Las Vegas, Nevada. http://crc.nv.gov.
[68] Shim, C., Wang, Y., Choi, Y., Palmer, P. I., Abbot, D. S., Chance, K. (2005): Constraining global isoprene emissions with Global Ozone Monitoring Experiment (GOME) formaldehyde column measurements. – J. Geophys. Res. 110: D24301. DOI: 10.1029/2004JD005629.
[69] Sippo, J. Z., Maher, D. T., Tait, D. R., Ruiz-Halpern, S., Sanders, C. J., Santos, I. R. (2016): Mangrove out welling is a significant source of oceanic exchangeable organic carbon. – Limnology and Oceanography Letters 2(1): 1-8.
[70] Souri, A. H., Choi, Y., Jeon, W., Woo, J.-H., Zhang, Q., J.-i. Kurokawa. (2017): Remote sensing evidence of decadal changes in major tropospheric ozone precursors over East Asia. – J. Geophys. Res. Atmos. 122: 2474-2492. DOI: 10.1002/2016JD025663.
[71] Stammes, P., Sneep, M., de Haan, J. F., Veefkind, J. P., Wang, P., Levelt, P. F. (2008): Effective cloud fractions from the ozone monitoring instrument: theoretical framework and validation. – J Geophy Res 113: D16S38. DOI: 10.1029/2007JD008820.
[72] Stavrakou, T., Müller, J.-F., Smedt, I. De., Van Roozendael, M., van der Werf, G. R., Giglio, L., Guenther, A. (2009): Global emissions of nonmethane hydrocarbons deduced from SCIAMACHY formaldehyde columns through 2003-2006 – Atmos. Chem. Phys. 9: 3663-3679. DOI: 10.5194/acp-9-3663-2009.
[73] Stavrakou, T., Müller, J.-F., Bauwens, M., De Smedt, I., Van Roozendael, M., Guenther, A., Wild, M., Xia, X. (2014): Isoprene emissions over Asia 1979-2012: impact of climate and land-use changes. – Atmos. Chem. Phys. 14: 4587-4605. 2014 www.atmos-chem-phys.net/14/4587/2014/. DOI: 10.5194/acp-14-4587-2014.
[74] Surl, L., Palmer, P. I., González Abad, G. (2018): Which processes drive observed variations of HCHO columns over India? – Atmos. Chem. Phys. 18: 4549-4566. https://doi.org/10.5194/acp-18-4549-2018.
[75] Tariq, S., Ali, M. (2015): Spatio-temporal distribution of absorbing aerosols over Pakistan retrieved from OMI Onboard Aura Satellite. – Atmos Pollut Res. DOI: 10.5094/APR.2015.030.
[76] Tariq, S., ul-Haq, Z., Ali, M. (2015): Analysis of optical and physical properties of aerosols during crop residue burning event of October 2010 over Lahore, Pakistan. – Atmos Pollut Res. DOI: 10.1016/j.apr.2015.05.002.
[77] Tariq, S., ul-Haq, Z., Ali, M. (2016): Satellite and ground-based remote sensing of aerosols during intense haze event of October 2013 over Lahore, Pakistan. – Asia-Pac J Atmos Sci. DOI: 10.1007/ s13143-015-0084-3.


http://www.aloki.hu ● ISSN 1589 1623 (Print) ● ISSN 1785 0037 (Online)
DOI: http://dx.doi.org/10.15666/aeer/1705_1098911015

[78] ul-Haq, Z., Tariq, S., Ali, M., Mahmood, K., Batool, S. A., Rana, A. D. (2014): A study of tropospheric $NO_2$ variability over Pakistan using OMI data. – Atmospheric Pollution Research 5: 709-720. DOI: 10.5094/APR.2014.080.

[79] ul-Haq, Z., Tariq, S., Rana, A. D., Ali, M., Mahmood, K., Shahid, P. (2015): Satellite remote sensing of total ozone column (TOC) over Pakistan and neighbouring regions. – International Journal of Remote Sensing 36(4): 1038-1054. DOI: 10.1080/01431161.2015.1007255.

[80] ul-Haq, Z., Tariq, S., Ali, M., Rana, A. D., Mahmood, K. (2017): Satellite sensed tropospheric $NO_2$ patterns and anomalies over Indus, Ganges, Brahmaputra and Meghna river basins. – International Journal of Remote Sensing 38(5): 1423-1450. DOI: 10.1080/01431161.2017.1283071.

[81] ul-Haq, Z., Rana, A. D., Tariq, S., Mahmood, K., Ali, M., Bashir, I. (2018): Modeling of tropospheric $NO_2$ column over different climatic zones and land use/land cover types in South Asia. – Journal of Atmospheric and Solar-Terrestrial Physics 168: 80-99.

[82] UNEP (2008): United Nations Environment Programme and Development Alternatives. – South Asia Environment Outlook 2009: UNEP, SAARC and DA. United Nations Environment Programme (UNEP).

[83] US-EPA (2009): Assessment of the Impacts of Global Change on Regional U.S. Air Quality: A Synthesis of Climate Change Impacts on Ground-Level Ozone. – US EPA, Washington, DC.

[84] van Vuuren, D. P., Edmonds, J., Kainuma, M., Riahi, K., Thomson, A., Hibbard, K., Hurtt, G. C., Kram, T., Krey, V., Lamarque, J.-F., Masui, T., Meinshausen, M., Nakicenovic, N., Smith, S. J., Rose, S. K. (2011): The representative concentration pathways: an overview. – Clim. Change 109: 5-31.

[85] Varotsos, C., Cartalis, C., Feidas, C., Gerasi, E., Asimakopoulos, D. N. (1992): Relationship of ozone and its precursors in the West Coast Air Basin of Athens: a statistical model for the assessment of air quality in an urban area. – Atmos. Res. 28: 41-47.

[86] Verma, A. K., Saxena, A., Khan, A. H., Sharma, G. D. (2015): Air pollution problems in Lucknow City, India: a review. – J. Environ. Res. Develop. 9(4): April-June.

[87] Voulgarakis, A., Savage, N. H., Wild, O., Braesicke, P., Young, P. J., Carver, G. D., Pyle, J. A. (2010): Interannual variability of tropospheric composition: the influence of changes in emissions, meteorology and clouds – Atmos. Chem. Phys. 10: 2491-2506. DOI: 10.5194/acp-10- 2491-2010.

[88] Wiedinmyer, C., Tie, X., Guenther, A., Neilson, R., Granier. C. (2006): Future changes in biogenic isoprene emissions: how might they affect regional and global atmospheric chemistry? – Earth Interactions 10: 3.

[89] Wolfe, G. M., Kaiser, J., Hanisco, T. F., Keutsch, F. N., de Gouw, J. A., Gilman, J. B., Graus, M., Hatch, C. D., Holloway, J., Horowitz, L. W., Lee, B. H., Lerner, B. M., Lopez-Hilifiker, F., Mao, J., Marvin, M. R., Peischl, J., Pollack, I. B., Roberts, J. M., Ryerson, T. B., Thornton, J. A., Veres, P. R., Warneke, C. (2016): Formaldehyde production from isoprene oxidation across $NO_x$ regimes, – Atmos. Chem. Phys. 16: 2597-2610.

[90] Yoo, J-M., Lee, Y. R., Kim, D., Jeong, M-J., Stockwell, W., Kundu, K., Prasun., Soo-Min, O., Dong-Bin, S., Lee, Suk-Jo, L. (2014): New indices for wet scavenging of air pollutants (O3, CO, NO2, SO2, and PM10) by summertime rain. – Atmospheric Environment 82. 226-237. 10.1016/j.atmosenv.2013.10.022.

[91] Zara, M., Boersma, K. F., De Smedt, I., Richter, A., Peters, E., van Geffen, J. H. G. M., Beirle, S., Wagner, T., Van Roozendael, M., Marchenko, S., Lamsal, L. N., Eskes, H. J. (2018): Improved slant column density retrieval of nitrogen dioxide and formaldehyde for OMI and GOME-2A from QA4ECV: intercomparison, uncertainty characterisation, and trends. – Atmos. Meas. Tech. 11: 4033-4058. https://doi.org/10.5194/amt-11-4033-2018.


http://www.aloki.hu ● ISSN 1589 1623 (Print) ● ISSN 1785 0037 (Online)
DOI: http://dx.doi.org/10.15666/aeer/1705_1098911015

[92] Zhang, J., Song, F., Tao, J., Zhang, Z., Shi, S. Q. (2018): Research Progress on Formaldehyde. Emission of Wood-Based Panel. – International Journal of Polymer Science Art. ID 9349721. https://doi.org/10.1155/2018/9349721.

[93] Zhu, L., Jacob, D. J., Mickley, L. J., Marais, E. A., Cohan, D. S., Yoshida, Y., Duncan, B. N., Abad, G. G., Chance, K. V. (2014): Anthropogenic emissions of highly reactive volatile organic compounds in eastern Texas inferred from oversampling of satellite (OMI) measurements of HCHO columns – Environ. Res. Lett. 9: 114004. DOI: 10.1088/1748-9326/9/11/114004.

[94] Zhu, L., Jacob, D. J., Kim, P. S., Fisher, J. A., Yu, K., Travis, K. R., Olfe, G. M. (2016): Observing atmospheric formaldehyde (HCHO) from space: validation and intercomparison of six retrievals from four satellites (OMI, GOME2A, GOME2B, OMPS) with SEAC$^4$RS aircraft observations over the Southeast US. – Atmospheric chemistry and physics 16(21): 13477-13490. DOI: 10.5194/acp-16-13477-2016.

[95] Zhu, L., Jacob, D. J., Keutsch, F. N., Mickley, L. J., Scheffe, R., Strum, M., Abad, G. G., Chance, K., Yang, K., Rappenglück, B., Millet, D. B., Baasandorj, M., Jaeglé, L., Shah, V. (2017): Formaldehyde (HCHO) As a hazardous air pollutant: mapping surface air concentrations from satellite and inferring cancer risks in the United States. – Environmental Science & Technology 51(10): 5650-5657. DOI: 10.1021/acs.est.7b01356.

[96] Zhu, S., Li, X., Yu, C., Wang, H., Wang, Y., Miao, J. (2018): Spatiotemporal variations in satellite-based formaldehyde (HCHO) in the Beijing-Tianjin-Hebei Region in China from 2005 to 2015. – Atmosphere 9: 5.


http://www.aloki.hu ● ISSN 1589 1623 (Print) ● ISSN 1785 0037 (Online)
DOI: http://dx.doi.org/10.15666/aeer/1705_1098911015